Transcriptomic analysis reveals a role for the nervous system in regulating growth and development of *Fasciola hepatica* juveniles

Emily Robb[1*], Erin McCammick[1*], Duncan Wells[1], Paul McVeigh[1], Erica Gardiner[1], Rebecca Armstrong[1], Paul McCusker[1], Angela Mousley[1], Nathan Clarke[1], Nikki Marks[1] and Aaron G. Maule[1*]

1. Microbes & Pathogen Biology, The Institute for Global Food Security, School of Biological Sciences, Queen's University Belfast, Belfast, United Kingdom

* Corresponding authors contributed equally to manuscript

Email: a.maule@qub.ac.uk

Email: e.robb@qub.ac.uk

Abstract

Fasciola spp. liver fluke have significant impacts in veterinary and human medicine. The absence of a vaccine and increasing anthelmintic resistance threaten sustainable control and underscore the need for novel flukicides. Functional genomic approaches underpinned by *in vitro* culture of juvenile *Fasciola hepatica* facilitate control target validation in the most pathogenic life stage. Comparative transcriptomics of *in vitro* and *in vivo* maintained 21 day old *F. hepatica* finds that 86% of genes are expressed at similar levels across maintenance treatments suggesting commonality in core biological functioning within these juveniles. Phenotypic comparisons revealed higher cell proliferation and growth rates in the *in vivo* juveniles compared to their *in vitro* counterparts. These phenotypic differences were consistent with the upregulation of neoblast-like stem cell and cell-cycle associated genes in *in vivo* maintained worms. The more rapid growth/development of *in vivo* juveniles was further evidenced by a switch in cathepsin protease expression profiles, dominated by cathepsin B in *in vitro* juveniles and then by cathepsin L in *in vivo* juveniles. Coincident with more rapid growth/development was the marked downregulation of both classical and peptidergic neuronal signalling components in *in vivo* maintained juveniles, supporting a role for the nervous system in regulating liver fluke growth and development. Differences in the miRNA complements of *in vivo* and *in vitro* juveniles identified 31 differentially expressed miRNAs, notably *fhe-let-7a-5p*, *fhe-mir-124-3p* and, miRNAs predicted to target Wnt-signalling, supporting a key role for miRNAs in driving the growth/developmental differences in the *in vitro* and *in vivo* maintained juvenile liver fluke. Widespread differences in the expression of neuronal genes in juvenile fluke grown *in vitro* and *in vivo* expose significant interplay between neuronal signalling and the rate of growth/development, encouraging consideration of neuronal targets in efforts to dysregulate growth/development for parasite control.

Author Summary

Parasitic worms are notoriously difficult to study outside of a host organism. However, recent developments in culture methods for *Fasciola hepatica* liver fluke juveniles support growth and development of these parasites in the laboratory (*in vitro*) towards adult parasites. Having the ability to grow pathogenic juvenile stages *in vitro* enables functional studies to validate potential drug and vaccine targets. However, comparison of *in vitro* grown juveniles to juveniles retrieved from infected hosts (*in vivo*) shows considerable size differences suggesting at least some differences in biology that could undermine the relevance of data generated from *in vitro* maintained parasites. This study examines gene expression differences between *in vitro* and *in vivo* maintained *F. hepatica* juveniles via transcriptomic analysis to identify similarities and differences in their biology which may help explain differences in the rate of growth and development. 86% of genes were shown to be expressed at similar levels across treatment groups suggesting a high level of biological similarity between *in vitro and in vivo* juveniles. However, the genes that are expressed differently between these juveniles will help improve current culture methods and provide a new group of potential drug targets that impact on juvenile growth and development.

Introduction

Fasciola spp. liver fluke are important helminth pathogens with far reaching global impacts on veterinary and human medicine causing a disease known as fasciolosis [1]. Global agricultural losses associated with *Fasciola* infection are estimated at around US$3.2 billion annually [2], although this is thought to be a considerable underestimation as *F. hepatica* parasites in particular are known to infect a wide range of mammalian hosts across broad geographical ranges [3, 4]. Designated a neglected tropical disease by the World Health Organisation (WHO) [1] due to its impact on human populations, *F. hepatica* is thought to infect up to 17 million people, with a further 91 million people at risk of infection worldwide [5].

Treatment of the early pathogenic stages of fasciolosis relies on the drug Triclabendazole, since other flukicides cannot kill young juveniles [4, 6]. Definitive mammalian hosts are infected through the ingestion of infectious metacercariae encysted on vegetation [7, 8]. Newly excysted juveniles (NEJs) emerge in the duodenum and migrate through the intestinal wall to the liver parenchyma, causing acute stages of disease associated with host blood loss and even death with high burden infections [7-9]. Although adults residing in the bile duct are reproductively active and associated with chronic infection, the major pathology associated with fasciolosis is caused by juvenile migration within the first few weeks of infection [10, 11]. The absence of a liver fluke vaccine and increasing anthelmintic resistance threaten the sustainability of liver fluke control. Triclabendazole treatment failure is widely reported for livestock and more recent cases of emerging resistance in human populations is deeply concerning and highlights the pressing need for new flukicides, particularly targeting the highly pathogenic early-stage juveniles [4, 12-14].

Despite the pathology associated with early-stage infections, there is a dearth of information on the biology of migrating juveniles due to their small size, liver parenchyma location and, historically, the absence of readily amenable *in vitro* culture methods [15]. At this stage of development, juveniles are growing and moving rapidly through host tissues, encountering different microenvironments and host responses [11]. Understanding the biology of these

behaviours and host-parasite interactions will support new target discovery and control option developments. Research into helminth infections often relies on the use of animal models to inform host-parasite relationships. However, such studies are often challenging, of variable relevance to livestock/human hosts and provide limited opportunity to interrogate parasite biology [16]. *In vitro* culture, where possible, supports curiosity driven research and provides many advantages to early-stage studies of parasite biology. However, despite recent advances in propagation of the full life cycle of *Schistosoma mansoni* [17], *in vitro* parasite culture is notoriously difficult and, where it is possible, the approaches need to reasonably replicate *in vivo* parasite biology such that readouts have relevance to control.

McCusker *et al.* [15] developed a chicken serum-based culture platform that promotes sustained *F. hepatica* juvenile survival, growth and development *in vitro*. This has facilitated the development of a robust functional genomics platform that promotes discovery-based studies that seed drug target identification and validation in the most damaging life stage [18]. Although extremely robust, the current culture platform is believed to support a slower rate of growth and development of *F. hepatica* juveniles *in vitro* when compared to *in vivo* counterparts and, whilst *in vitro* juveniles start to develop adult like features, they do not progress to egg laying adults [15]. In the absence of culture methods that allow full life cycle propagation, it is important to ascertain if the slower growing *in vitro* worms resemble their *in vivo* counterparts to ensure functional genomics studies on *in vitro* cultured juveniles have relevance to control.

Taking advantage of recent developments in genomic and transcriptomic resources for *F. hepatica*, we present in depth comparative transcriptomic analysis of 21 day *in vitro* maintained *F. hepatica* juveniles and stage matched 21 day *in vivo F. hepatica* juveniles, describing key differences in gene expression in the most pathogenic life stage under differing growth conditions. Although the expression of core biological functioning components is consistent in comparisons between the two growth conditions, the differences that are evident can mostly be explained by the disparate rates of growth and cell proliferation observed in the

two groups. Notably, protease expression profiles differ and corroborate the hypothesis that time-matched *in vitro* maintained juveniles develop more slowly than *in vivo* juveniles, such that when time-matched, the *in vitro* juveniles are at an earlier stage of development. The data indicate a key role for miRNAs in driving the developmental differences between *in vitro* and *in vivo* maintained juveniles with over one third of the identified miRNAs being differentially expressed. Further, profound differences in the expression of genes associated with neoblast proliferation and development are consistent with the observed higher rate of neoblast-like stem cell proliferation *in vivo*. The unexpected down-regulation of multiple nervous system associated signalling pathways exposes an important role for the nervous system of *F. hepatica* in the modulation of juvenile growth and development, encouraging efforts to identify neuronal signalling pathways that dampen cell proliferation and/or growth dynamics.

Results

A total of 30,892 transcripts were identified from this analysis (S1 Text) which were further refined to define a dataset of 19,343 unique genes for 21 day old juvenile *F. hepatica* (removal of transcript isoforms and non-zero read counts from *in vitro* and *in vivo* assembled transcriptomes) reflective of the greatest depth of sequencing achieved to date for *F. hepatica* (average 252 million mapped reads per replicate transcriptome, S2 Table) [19-23]. All genes were annotated using a core annotation pipeline described in Fig 1. Annotations were assigned to 64% (12,300) of genes based on matches from at least one database interrogated (S3 Table).

Differentially expressed genes within these datasets offer insight into the biological differences of juveniles under distinct maintenance conditions and have the potential to identify ways in which *in vitro* culture methods could be improved. Since a primary phenotypic difference between *in vitro* and *in vivo* maintained juveniles is worm size, with age-matched *in vivo* juveniles being ~15-times larger (Fig 2A-C), it can be hypothesized that differentially expressed genes play roles in the growth and development of juveniles; these genes have the potential to seed the identification of targets critical to pathogen virulence and establishment within the host. Staining proliferating cells of juveniles in both growth conditions using 5-ethynyl-2-deoxyuridine (EdU) revealed increased EdU+ cells in *in vivo* maintained juveniles (18859±1388 Edu+ cells after 18 h; n=4; Fig 2B) when compared to *in vitro* counterparts (316±30 Edu+ cells after 18 h; n=26; Fig 2A), revealing a 60-fold difference in the number of proliferating cells. The enhanced cell proliferation in *in vivo* juveniles was also evident when data were normalised to account for the ~15-fold size difference (Fig 2C), confirming that the larger worms were supported by a ~4-fold higher rate of cell proliferation.

Differential expression of genes associated with selected cellular processes

DESeq2 was used to analyse differential expression of genes between *in vitro* and *in vivo* treatments. Analysis identified 1339 genes upregulated (6.9%) and 1320 genes downregulated (6.8%) *in vivo* compared to *in vitro* counterparts, amounting to a total of 13.7% of expressed genes being differentially expressed between maintenance treatments (Fig 2D). Annotations were assigned to 72% (1923) of differentially expressed genes from at least one hit match from interrogated databases of the annotation pipeline (S3 Table).

Notably, Gene Ontology (GO) term analysis highlighted an increase in cellular processes associated with DNA replication in datasets of *in vivo* maintained worms with an increased number of the genes associated with transcription regulation, DNA replication and microtubule based processes/movement compared to *in vitro* maintained worms (Fig 3A&B). Genes associated with nuclear based cellular components (nucleus, microtubules, MCM complex, chromosome, nucleosome) were also upregulated *in vivo* (Fig 3C). Although KEGG pathway analysis showed similar results, it more specifically highlighted a significant upregulation of genes associated with cell cycle, meiosis and cellular senescence pathways *in vivo* (Fig 3D) - all processes associated with cell division. GO term analysis of *in vitro* maintained juvenile datasets highlighted a more diverse range of gene functions. Genes associated with oxidation-reduction processes were upregulated in *in vitro* juvenile datasets suggesting some metabolomic differences between treatment groups, whilst an increased number of genes associated with transmembrane transport, G protein signalling and ion transport suggested an enhancement of some cell signalling pathways in *in vitro* juveniles when compared to *in vivo* counterparts (Fig 3A-C). KEGG enrichment analyses showed a significant downregulation of genes associated with the synaptic vesicle cycle, axon guidance and, more specifically, cholinergic signalling *in vivo* (Fig 3D). N glycan biosynthesis and protein processing in the endoplasmic reticulum were also significantly downregulated *in vivo* compared to *in vitro* maintained juveniles, interesting as glycosylation has been proposed to play a significant role in host-parasite interaction and suggests that glycosylation is an important protein modification within *in vitro* juveniles (Fig 3D). An increase in lysosomal

pathway genes in *in vitro* maintained juveniles may be associated with the prevalence of cathepsin B proteases with greater homology to human proteases than the cathepsin L proteases that were more abundant in *in vivo* datasets. Cathepsin profiles are discussed in more detail later.

Cell cycle- and neoblast-associated genes are upregulated in in vivo *maintained juveniles*

Eighty nine percent (17,166) of total genes identified are found in all datasets (Fig 4A; 3x *in vitro*= 21d_ivt1-3; 3x *in vivo*= 21d_ivv1-3). In addition to differentially expressed genes, those genes which are present in only one treatment group, *i.e.* genes considered switched 'on' or 'off' *in vivo* are also genes of interest for understanding mechanisms of juvenile growth and development. Unsurprisingly, more genes (226; S3 Table) are present only in *in vivo* datasets, likely due to the demands of a more complex and changing host environment (S3 Table). 76/226 genes returned no hits when interrogated against the databases of the annotation pipeline, suggesting these genes are novel and unique to *in vivo F. hepatica* juveniles. 'Hypothetical protein' annotations were assigned to 65 genes and 85 genes were allocated function using the annotation pipeline described. A significant proportion of the genes only identified *in vivo* are associated with cell cycle processes and transcription regulation including cyclin-dependent kinase, cyclin, centromere protein, nucleosome assembly protein, transcription factors and zinc finger proteins (S3 Table). Also present only in *in vivo* datasets are genes associated with cell structure such as centrin, tubulins (alpha and beta chains) and actin associated proteins (slingshot protein phosphatase and actin-interacting protein) involved in microtubule and microfilament formation. Increased expression of these genes in the *in vivo* datasets is consistent with increased cell proliferation and turnover in these juveniles. Only 64 genes were present solely in *in vitro* datasets; 24 of these were assigned function using the annotation pipeline (S3 Table). Although no clear pattern of gene groups was evident, a histone 2B gene commonly associated with cell proliferation was within the *in vitro*-only datasets, suggesting that it could be associated with an earlier stage of growth and

development in *F. hepatica* juveniles or is linked to an unknown feature of *in vitro* juvenile biology.

Closer examination of all cell cycle-associated genes shows a high proportion of these genes upregulated *in vivo* across all cell-cycle stages, corroborating an increased rate of cell division in these juveniles (Fig 4B). In particular, all components of the highly conserved MCM2-7 complex and cell division cycle genes (*cdc-6, cdc-45, cdc-25*) known to tightly regulate key components of DNA replication (Fig 4B). Key regulators of cell cycle progression, including cyclins and cyclin-dependent kinases (CDKs), are also significantly upregulated suggesting cell cycle activities are occurring at an increased rate *in vivo* (Fig 4B). The kinases polo-like kinase-1 (*plk-1*) and aurora-b kinase (*aurkb*), thought to ensure accurate chromosomal segregation, were also upregulated *in vivo*, which would appear to be consistent with the phenotypic observations (Fig 4B). To characterise further the relationship between growth/development and neoblast-like stem cells, differential expression analysis considered the 128 neoblast-like cell markers identified in *S. mansoni* [24]. Of these genes, 108 were found to have orthologues in the *F. hepatica* genome and 53 were shown to be differentially expressed and upregulated in *in vivo* maintained juveniles (S4 Table), consistent with the altered stem cell dynamics needed to drive faster growth and development in these juveniles (Fig 4C; S4 Table). Amongst the known neoblast markers significantly upregulated in the *in vivo* juveniles were the key transcriptional regulators *nanos* (3 genes) and *sox-1,* previously identified as being essential for neoblast proliferation in flatworms [24, 25] (Fig 4C). These data offer new insight into important genes regulating essential mechanisms of *F. hepatica* growth and development and provide a starting point for functional validation as potential control targets.

Protease profile dynamics differ within the in vitro and in vivo maintained juveniles

Cathepsin (CAT) proteases represent >80% of the proteins secreted by adult liver fluke [26] and are of particular interest due to their role at the host parasite interface and potential in vaccine development [26-29]. CATs display marked temporal changes in expression during juvenile fluke development associated with altering proteolytic requirements of the parasite as it migrates within the mammalian host [26, 28]. 34 potential CATs (23 CATL and 11 CATB) have been previously described within the *F. hepatica* genome [26]. Our datasets, suggest that *F. hepatica* in fact express 43 individual CAT (29 CATL and 14 CATB) proteins (S4 Table). It should be noted that two novel gene sequences (MSTRG.20621; MSTRG.9158) identified through this analysis align well with previously annotated CATs (maker-scaffold10x_895_pilon-snap-gene-0.1; maker-scaffold10x_250_pilon-snap-gene-0.13), however, these novel sequences are significantly truncated at their N terminus suggesting they may have distinct functions. Annotated separately in this analysis, it is also possible these genes are isoforms of previously annotated genes which would bring the overall cohort of *F. hepatica* CAT genes down to 41 (27 CATL and 14 CATB). Of the 43 CATs identified from this analysis, 32 genes were differentially expressed suggesting that CAT profiles of *in vitro* and *in vivo* maintained juveniles are considerably different (Fig 5A). 22 CATLs were differentially expressed, of which 14 were upregulated *in vivo* (Fig 5A; left; S4 Table). One novel gene, MSTRG.9158 was identified as the most upregulated *in vivo* ($Log_2FC=17.46$) and found to be a truncated CATL1 protein with high similarity to maker-scaffold10x_250_pilon-snap-gene-0.13. There was a general trend of CATL1 genes (including MSTRG.9158) being upregulated *in vivo*. SignalP (v.5.0) analysis of upregulated cathepsins showed 80% contained a signal peptide, suggesting they may be secreted at the host-parasite interface (S4 Table). CATL encoding genes downregulated *in vivo* are thought to belong to clade 5, suggesting these cathepsins in particular are more important in biology associated with *in vitro* maintenance (S4 Table). Ten CATB proteins were differentially expressed, 9 of these were downregulated *in vivo* 21 day-old worms (Fig 5A; left; S4 Table); 2 novel CATB proteins not previously annotated were identified (MSTRG.21893 and MSTRG.6836). The downregulation of CATB genes *in vivo* was also correlated with a downregulation of legumain regulatory peptidases, likely

relating to the *trans*-activation of CATB proteases by legumains (Fig 5B). These data suggest CATB proteases are more important to the biology of *in vitro* maintained juveniles, whilst CATL proteases are more significant in the biology of *in vivo* maintained juveniles, likely due to host interactions. It is possible that the differences in cathepsin expression relate to developmental differences between the two treatment groups – indeed, a switch from CATB protease expression to CATL expression has been linked with the development of *F. hepatica* juveniles *in vivo* [26, 28]. To investigate this hypothesis the expression of CAT genes annotated in the genome (PRJEB25283, WBPS14; 21 CATL and 8 CATB genes) was correlated with expression in the previously published life stage transcriptomes, with a specific focus on newly excysted juvenile (NEJ), 24 hour juvenile and adult datasets (Fig 5A). These data show a general trend of CATs upregulated *in vivo* showing greater expression in the juvenile and adult stages of development, whilst the CAT genes downregulated *in vivo* show greater expression in the 24 hour NEJ stage of development (Fig 5A). These observations are consistent with a developmental delay in the *in vitro* maintained juveniles compared to their age matched *in vivo* juveniles. Anomalies in the pattern show some genes downregulated *in vivo* have higher expression in juvenile/adult datasets (CAT-B; maker-scaffold10x_1382_pilon-snap-gene-0.52 and maker-scaffold10x_889_pilon-snap-gene-0.31, CAT-L; maker-scaffold10x_231_pilon-augustus-gene-0.4) and some genes upregulated *in vivo* have greater expression in NEJ datasets (CATL; maker-scaffold10x_1853_pilon-snap-gene-0.17). This is likely due to the *in vitro* juveniles being significantly more developed than 24 hour NEJs and the *in vivo* juveniles expressing a mix of cathepsin B and cathepsin L proteins as they transition towards the adult life-stage. Other protease expression dynamics included an increased proportion of metalloproteinases in the *in vivo* juveniles, likely to aid in host tissue degradation (Fig 5B). There was an increased proportion of calpain proteases in the *in vitro* juveniles, consistent with observations in *Schistosoma* spp. where they are important for early juvenile migration and host evasion due to their role in immune defence [30].

297 *Metabolomic differences between in vitro and in vivo maintained F. hepatica juveniles*

298 Parasitic flatworms rely heavily on carbohydrate substrates for energy metabolism [31]. *F.*
299 *hepatica* have been shown to switch from aerobic energy metabolism via aerobic acetate
300 production using the Tricarboxylic Acid Cycle (TCA) pathway, to anaerobic dismutation [20,
301 31] as they transition from free living to parasitic life stages. *In vitro* cultured juveniles are
302 maintained under anaerobic conditions long term (5% CO_2), but given the opportunity can also
303 undergo aerobic metabolism, whilst 21 day *F. hepatica* juveniles burrowing through the liver
304 parenchyma are undergoing a switch to predominantly anaerobic metabolism. Surprisingly,
305 the key enzymes (pyruvate kinase, Fh-PK; succinate dehydrogenase, Fh-SD; malic enzyme,
306 Fh-ME; phosphoenolpyruvate carboxykinase, Fh-PEPCK) associated with all pathways of
307 carbohydrate metabolism (aerobic and anaerobic) are downregulated *in vivo,* suggesting
308 enhanced metabolic activities, both aerobic and anaerobic, in the *in vitro* maintained juveniles
309 (Fig 5C). The upregulation of lactate dehydrogenases in *in vitro* datasets suggests these
310 juveniles are generating greater levels of lactate metabolic waste than *in vivo* juveniles, whilst
311 the upregulation of acetate:succinate CoA-transferase in *in vivo* juveniles suggests that they
312 are producing higher levels of acetate (S4 Table). To investigate this further, *in vitro*
313 maintained juveniles were maintained in an anaerobic chamber, removing the ability to
314 undergo aerobic respiration. These juveniles were unable to grow and showed declining
315 health across a two week period when compared to juveniles maintained under 5% CO_2
316 conditions (S5 Fig). After 3 weeks, significant death (87.4%) resulted in termination of the
317 experiment.

318

319 *N-glycan biosynthesis and processing enzymes downregulated in vivo*

320 KEGG pathway analysis highlighted the downregulation of genes associated with N-glycan
321 biosynthesis and processing *in vivo* (Fig 3D). On closer examination of protein glycosylating
322 genes described by McVeigh et al. [32], downregulation *in vivo* is particularly associated with

components of the oligosaccharyl transferase (OST) complex involved in the *en-bloc* transfer of glycans to proteins [33], including catalytic core domain proteins STT3A/STT3B and RPN-1/-2 proteins (S5 Fig). Glycans are commonly linked to roles in host parasite interactions [34, 35] and the high expression of glycosylating enzymes associated with glycan biosynthesis in *in vitro* maintained worms suggests that aspects of host-parasite interactions are sustained *in vitro* even in the absence of a host. It is important to note that there was no differential expression of O-linked glycosylation genes, again thought to correlate with host-parasite interactions [34, 35].

Components of the F. hepatica nervous system are downregulated in vivo

KEGG pathway analysis highlighted a significant downregulation of nervous system components *in vivo*. Flatworms employ both classical and neuropeptidergic neurotransmitters for neurotransmission [36-38] and both displayed markedly reduced expression in the *in vivo* juveniles (Fig 6).

The synaptic vesicle cycle is responsible for packaging and releasing neurotransmitters from the synapse to modulate neurotransmission [39]. All major components of this pathway were significantly downregulated *in vivo* suggesting an increased rate of neurotransmitter release, and as a result, classical neurotransmission communication in *in vitro* maintained juveniles (Fig 6A; top). Further examination revealed downregulation of the cholinergic signalling pathway and a noteworthy partial downregulation of the glutamate-signalling pathway, emphasising the importance of these two pathways to the biology of *in vitro* maintained juveniles (Fig 6A; bottom). Although classical neurotransmission is most commonly associated with modulating neuromuscular control in parasitic flatworms [40], these data suggest a novel role in growth and development. The majority of genes associated with serotonin and dopamine classical neurotransmitter signalling pathways were not differentially expressed. Serotonin has been highlighted as an essential component of the *F. hepatica*

nervous system with a core role in neuromuscular control [41, 42] - its stable expression across treatments suggests some core functioning of the liver fluke nervous system were not changed by maintenance treatment.

Interestingly, major components of neuropeptide signalling were also downregulated *in vivo* with the entire neuropeptide processing pathway displaying reduced expression [37]. Genes encoding two signal peptidases, prohormone convertase-2 (*PC-2*), carboxypeptidase E (*CPE*), peptidylglycine α-hydroxylating monooxygenase (*PHM*) and peptidyl-alpha-hydroxyglycine alpha-amidating lyase (*PAL*) were all downregulated *in vivo* (Fig 6B). The downregulation of neuropeptide processing suggests neuropeptides are being produced at a decreased rate *in vivo* compared with *in vitro* maintained juveniles, suggesting neuropeptide signalling displays changing expression dynamics during development. We identified 35 neuropeptide (*npp*)-encoding genes in the *F. hepatica* genome (PRJEB25283, WBPS14) and 17 *npp*-encoding genes were differentially expressed between maintenance treatments; all 17 were significantly downregulated in the *in vivo* juveniles compared to *in vitro* juveniles (S4 Table), corroborating the hypothesis that neuropeptide signalling is increased in the *in vitro* maintained juveniles and may play a previously undescribed role in modulating liver fluke growth and development. 6 *npp*-encoding genes were downregulated *in vivo* with a $\log_2$FC <-2 and are of particular interest as potential modulators of growth and development in *F. hepatica* juveniles. Two of the most significantly downregulated *npp*-encoding genes are NPF/NPY neuropeptides, homologous to vertebrate NPY neuropeptides (S4 Table) [38, 43]. McVeigh et al. [44] identified 35 *F. hepatica* G-protein coupled receptors (GPCRs). Combining available genomic and transcriptomic datasets suggests *F. hepatica* expresses 44 peptide GPCRs, of which 15 are differentially expressed (S4 Table). Ten peptide GPCRs were downregulated *in vivo* and one of these was previously hypothesized to be an NPY receptor. Further, 5 peptide GPCRs were downregulated in the *in vitro* juveniles, corroborating KEGG pathway analysis which suggests GPCR signalling is relatively higher in the *in vitro* maintained juveniles. These observations support the hypothesis that selected classical

neurotransmitters and neuropeptides act to modulate growth and development of *F. hepatica* juveniles, warranting further experimental exploration.

MicroRNAs (miRNA) are differentially expressed in in vitro and in vivo maintained juveniles

This study identified 103 miRNAs in liver fluke, including 14 novel miRNAs (S6 Table) and 89 miRNAs reported in previous studies on *F. hepatica* [45-49]. Recently, Herron et al [49] highlighted considerable redundancy across published miRNAs and moved to refine the current cohort of F*. hepatica* miRNAs by removing duplicate sequences of high similarity and retaining the longer sequence as individual miRNAs. Applying this approach to our dataset refines our final miRNA dataset to 89 miRNAs (75 previously published [45-49]; 14 novel). Of the 89 total miRNAs described for *F. hepatica*, 31 were differentially expressed between *in vivo* and *in vitro* maintained juveniles; 18 miRNAs were significantly upregulated in *in vivo* juveniles and 13 were significantly downregulated in *in vivo* juveniles, suggesting a role for these miRNAs in transcriptional regulation across maintenance conditions (Fig 7A). Gene ontology (GO) term analysis of predicted gene targets for differentially expressed miRNAs shows the increased expression of mRNA targets associated with transcriptional regulation, microtubule-based processes and DNA replication, whereas predicted mRNA targets associated with transmembrane transport, ion transport and signal transduction were downregulated in *in vivo* juveniles (Fig 7B). These data correlate with mRNA analysis and suggest these processes are at least partially regulated by miRNAs in liver fluke. Notably, Wnt signalling was identified as a process likely to be impacted by differentially expressed miRNAs with upregulated miRNAs (*fhe-mir-10-5p*, *fhe-mir-190-5p*, *fhe-mir-2b-3p*, *fhe-pubnovelmiR-23-3p*, *fhe-novelmir-50-5p*, *fhe-novelmir-28-3p*) predicted to target Wnt-associated genes that displayed reduced expression in *in vivo* maintained juveniles (Fig 7, S6 Table). Five Wnt genes downregulated in *in vivo* juveniles were predicted as regulated by miRNAs (2 Wnt proteins, maker-scaffold10x_735_pilon-snap-gene-0.38 & maker-scaffold10x_254_pilon-augustus-gene-0.12; 1 secreted frizzled-related protein, maker-

403 scaffold10x_405_pilon-snap-gene-0.20; 2 frizzled GPCRs, maker-scaffold10x_541_pilon-
404 snap-gene-0.38 & maker-scaffold10x_944_pilon-snap-gene-0.48). Three downregulated
405 miRNAs (*fhe-novelmir-48-3p*, *fhe-mir-184-5p* & *fhe-pubnovelmir-22-3p*) were also predicted
406 to target low-density lipoprotein receptor-related protein (LRP) 5/6 (maker-
407 scaffold10x_442_pilon-snap-gene-0.18), a Wnt-associated gene upregulated in *in vivo*
408 maintained juveniles (Fig. 7, S6 Table).
409
410 Two downregulated miRNAs were more significantly differentially expressed than others, *fhe-*
411 *mir-124-3p* identified by Fontenla et al. [47] and *fhe-pubnovelmir-22-3p* identified by Fromm
412 et al. [46] (Fig 7A). In contrast *fhe-let-7a-5p,* first identified by Fromm et al. [46] and considered
413 a highly conserved miRNA, was the most significantly upregulated miRNA in *in vivo*
414 maintained juveniles, whilst *fhe-novelmir-55-3p* identified from this study was the most
415 upregulated miRNA (Log_2FC= 2.33) in the *in vivo* maintained juveniles (Fig 7A). Analysis
416 suggested that these four miRNAs play a significant role in regulating the expression of genes
417 associated with *in vitro* and *in vitro* survival. Differentially expressed predicted targets for
418 these miRNAs include transcription factors, cell cycle proteins, apoptosis inhibitors, growth
419 factors, metabolomic and glycosylating enzymes (S4 Table).
420
421

Discussion

To date, this is the most in depth transcriptomic study of *F. hepatica* juveniles, providing crucial datasets for understanding the biology of this pathogenic stage, improving understanding and informing drug target identification and validation efforts.

13.7% of genes were considered differentially expressed in this study, with >86% of genes expressed at similar levels in *in vitro* and *in vivo* maintained juveniles. This suggests that core biological functioning is consistent in juveniles under the two growth conditions and despite the size differences observed between juveniles, the current *in vitro* maintenance platform supports relevant biological processes [15]. This corroborates previous observations that *in vitro* maintained juveniles develop phenotypic attributes consistent with *in vivo* developing juveniles [15], supporting the value of the *in vitro* functional genomics platform for initial drug target validation studies prior to the use of animal models of infection. Although *in vitro* and *in vivo* juvenile biology appear largely consistent, it is clear that parasites are highly adaptive and respond rapidly to changing external conditions [50]. It is likely that *in vitro* maintained juveniles are not exposed to host-related triggers that enhance growth/development dynamics as observed in the *in vivo* juveniles. Studies of nematode parasites suggests that parasites undergoing tissue migration are likely to be larger than closely related species that do not migrate and showcase greater levels of growth and development, suggesting the action of migration itself can stimulate this biology [51].

Transcriptome differences between the *in vitro* and *in vivo* juveniles were consistent with the observed differences in the rate of cell proliferation. Genes associated with cell proliferation and known neoblast markers were significantly upregulated *in vivo*, correlating with larger juvenile size. Neoblasts have previously been associated with growth and development of many flatworm species, including *F. hepatica* and related *Schistosoma mansoni* [15, 24, 52-55]. In the cestode *Echinococcus multilocularis*, stem cells were shown to be the only cells driving metacestode growth and regeneration [55]. Again, this suggests proliferation at a

448 higher rate *in vivo* leading to more rapid development of these juveniles. The identification of
449 cues that further stimulate cell proliferation is key to improving the current *in vitro* culture
450 methods. In addition to the role in growth and development, neoblast proliferation has also
451 been associated with rapid tegumental renewal and tissue repair of parasites *in vivo*,
452 suggesting the importance of these cells to host-parasite interactions [56]. The tegument is
453 the barrier between host and parasite such that its rapid renewal allows parasites to counter
454 host immune responses through active evasion and/or repair of immune response-associated
455 damage [56]. Clearly, the upregulation of neoblast-associated genes *in vivo* may partly relate
456 to the demands of immune challenge and *in vivo* survival, challenges not faced during *in vitro*
457 culture. It is noteworthy that a higher rate of neoblast proliferation was associated with the
458 mitigation of tissue damage and crucial to *S. mansoni* survival *in vivo* [57].

459 Metabolomic differences in *in vitro* and *in vivo* juveniles may also help explain the observed
460 differences in juvenile growth and development. Surprisingly, highly expressed genes
461 associated with carbohydrate metabolism (aerobic and anaerobic) were upregulated in *in vitro*
462 maintained juveniles. It is possible that this observation relates to the fact that chicken serum
463 has a glucose content twice the level of that seen in mammals [58]; the increased expression
464 of genes associated with carbohydrate metabolism may reflect the juveniles taking advantage
465 of the higher substrate availability. During their development from NEJs to adult fluke, juvenile
466 *F. hepatica* are reported to display a shift from aerobic to anaerobic carbohydrate metabolism.
467 Early studies by Tielans *et al*. showed under aerobic conditions that juveniles transitioned from
468 metabolism dominated by the Krebs cycle in early parenchymal stages, to aerobic acetate
469 production dominating during later parenchymal stages, with malate dismutation being
470 dominant in the bile duct stages [59]. Although specific to aerobic conditions and likely not a
471 true representation of *in vivo* scenarios, our data appear consistent with a similar pattern of
472 development such that *in vitro* juveniles are undergoing metabolism more akin to earlier
473 parenchymal stages utilising glycolysis to produce high levels of lactate, whilst the *in vivo*
474 juveniles are generating acetate, akin to later parenchymal stages. Note that culturing

475 juveniles under anaerobic conditions led to the death of juveniles suggesting that even *in vivo,*
476 migrating juveniles continue aerobic metabolism. These observations were supported by the
477 fact there were no distinct differences in the expression of aerobic and anaerobic metabolism
478 genes between treatment groups.

479 The slower development of *in vitro* juveniles is also reflected in the expression patterns of
480 CATL and CATB proteases. It is well documented that juvenile fluke undergo a developmental
481 shift from CATB expression to CATL expression as they develop from NEJs in the duodenum
482 to adult liver fluke in the bile duct [26-28]. This is thought to reflect the changing protease
483 requirements associated with feeding and tissue degradation [26]. Our transcriptomic
484 datasets show greater expression of CATB proteases in the *in vitro* juveniles, reflective of
485 early stage *F. hepatica* juveniles, whilst CATLs are more prominent in the *in vivo* juveniles,
486 characteristic of later stages of development. The cathepsin profile developmental shift was
487 previously described as occurring in the absence of host signalling [20], suggesting that the
488 developmental delay of *in vitro* maintained *F. hepatica* juveniles is responsible for this
489 difference. It is also possible that host-derived triggers during migration drive the changing
490 cathepsin expression profiles seen in the *in vivo* juveniles. These data encourage further
491 studies comparing earlier *in vivo* juveniles and later *in vitro* juveniles to see if matching
492 cathepsin expression profiles could be a proxy for the alignment of *in vivo* and *in vitro*
493 developmental stage. In addition to cathepsins, other proteases thought to play roles in host-
494 parasite interactions, such as calpains, were also evident in the *in vitro* datasets [30].
495 Somewhat surprisingly, the proposed immunomodulatory protein helminth defence molecule
496 (HDM-1), was not differentially expressed between the *in vitro* and *in vivo* maintained juveniles
497 [60-62]. Indeed, the gene encoding HDM-1 had a raw gene count of >1 million in both
498 treatment groups.

499 Glycan biology is also considered key for host-parasite interactions [34]. Our analysis
500 revealed the consistent expression of proteins associated with O-linked glycosylation and the
501 higher expression of N-linked processing enzymes in *in vitro* maintained juveniles. The

specific relationship between N-glycans and *in vitro* maintained juveniles is unknown, but it is perhaps due to the availability of glucose in chicken serum, an important precursor of the N-linked glycan biosynthetic pathway [63]. It is also possible that these specific glycans are more important for some aspects of biology associated with *in vitro* culture of juveniles or are associated with host-parasite interactions at earlier stages of parasite development. These observations suggest that *in vitro* cultured *F. hepatica* juveniles have utility in informing aspects of the biology of genes involved in host-parasite interplay.

Major components of both classical and neuropeptidergic signalling pathways in the liver fluke nervous system were downregulated *in vivo,* including synaptic vesicle cycle components and all elements of the neuropeptide processing pathway, indicating that these pathways are more prominent in the biology of *in vitro* maintained worms. Acetylcholine signalling in particular was a significantly upregulated classical neurotransmitter pathway in *in vitro* maintained juveniles. Notably, both acetylcholine and NPF/NPY neuropeptides have been identified as functioning in behaviours associated with nutrient acquisition and feeding in invertebrate species [64-66]. Acetylcholine signalling has been shown to function in the modulation of glucose transport in *S. mansoni* [65], whilst Drosophila NPF functions downstream of insulin signalling to regulate larval feeding [67]. The upregulation of these pathways may reflect the contrasting nutrient availabilities, resulting in changing behaviours of nutrient acquisition that could impact the growth and development of juveniles.

Of particular interest is the hypothesis that these neuronal signalling systems play important roles in the modulation of growth and development of juvenile *F. hepatica* via mechanisms that influence stem cell dynamics and/or nutrient acquisition. Recent advances in cancer biology identifies acetylcholine receptors as key players in cancer development due to their modulatory role in cell proliferation and expression in non-neuronal cell types [68]. Receptors for acetylcholine have been identified in all human stem cell populations and in differentiated and undifferentiated cells types, supporting an important function beyond basic nervous system functioning towards determination of cell fate and proliferation [69, 70]. The role of

acetylcholine signalling in the growth and development of invertebrate species is unclear, although as early as 1985, the exogenous application of acetylcholine was reported to improve the growth and proliferation of *Drosophila* cell lines *in vitro* [71]. The activation of nicotinic acetylcholine receptors by the nicotinic agonist dimethylphenylpiperazinium (DMPP) resulted in delayed cell division and differentiation, stunting the development of *Caenorhabditis elegans* L2s via interaction with the insulin/IGF and Ras-MAPK growth signalling pathways [72]. Further, *in situ* hybridisation experiments showed the extensive expression of nicotinic acetylcholine receptors in developing *Brugia malayi*, suggesting a specific role in embryogenesis and spermatogenesis [73]. NPF/NPY neuropeptides have also been linked to the modulation of regeneration and germline cell proliferation in invertebrates [74-76]. Non-neuronal NPF neuropeptides were shown to regulate bone morphogenetic protein (BMP) signalling and act as a key regulator of mating-induced germline cell proliferation in *Drosophila* females [76]. In free living flatworms, NPF was found to accelerate pharyngeal regeneration in *Girardia tigrina* [77], whilst RNAi of prohormone convertase 2 (PC2) and non-neuronal NPY-8 had significant impacts on the reproductive maturation of *Schmidtea mediterranea*, suggesting neuropeptides are essential for germ cell differentiation [78]. It is therefore possible that differential expression of these neuronal signalling pathways relates to a fundamental role of the nervous system in regulating the growth and development of *F. hepatica* juveniles; the data would support the hypothesis that cell proliferation and/or related growth mechanisms are inhibited by a cadre of neuronal signalling molecules. It is also possible that an upregulation of neuronal signalling in *in vitro* juveniles may result from their maintenance in an unfamiliar environment lacking directional cues, heightening the expression of systems involved in host/niche finding behaviours.

miRNAs are an abundant class of regulatory genes that control many cellular and developmental processes [79]. Analysis of the miRNA complements of *in vitro* and *in vivo* maintained juvenile *F. hepatica* supports a significant role for these small RNAs in the modulation of developmental processes, including transcription and translation. The most

556 significantly upregulated miRNA in *in vivo* juveniles was *fhe-let-7a-5p;* this miRNA is highly
557 conserved across diverse organisms and has a significant role in the modulation of stem cells
558 and the promotion of cell differentiation [80,81], consistent with its upregulation in the more
559 highly developed *in vivo* maintained *F. hepatica* juveniles. *Fhe-mir-124-3p* plays a key role in
560 neuronal cell differentiation [82] and is also thought to be a growth suppressor [83], potentially
561 correlating with its higher expression in the smaller *in vitro F. hepatica* juveniles. The
562 downregulation of *fhe-mir-124-3p* in *in vivo* juveniles may reflect the developmental stage of
563 these juveniles with well-formed neuronal systems supported by comparatively lower levels of
564 neuronal development. It was notable that GO term analysis of predicted miRNA targets
565 largely correlated with the most significantly differentially expressed mechanisms identified
566 through mRNA transcriptome analysis. In addition, Wnt signaling was identified as a process
567 regulated by differentially expressed miRNAs leading to an overall downregulation of Wnt
568 mRNAs *in vivo.* miRNAs are well established regulators of Wnt signaling, a process essential
569 for early organism development [84]. Downregulation of specific Wnt proteins, secreted
570 frizzled-related proteins and frizzled GPCRs *in vivo,* suggest these proteins in particular have
571 key roles in early stage developmental processes, consistent with later stage juveniles
572 maintaining higher levels of tissue differentiation. Upregulation of low-density lipoprotein
573 receptor-related protein (LRP) 5/6, a Wnt-associated gene, in *in vivo* juveniles suggests this
574 protein is involved in later stage developmental processes.

575 Overall, this study has provided unique insight into the biology of a helminth parasite
576 maintained *in vitro* and encourages the exploitation of *in vitro* cultured parasites in functional
577 genomics studies to inform aspects of *in vivo* biology and control target validation. Where
578 biology differs in relation to growth and development, new insights into metabolomic
579 differences offer a basis for improving *in vitro* culture methods towards identifying key triggers
580 for adult fluke development. Most of the transcriptomic differences between *in vitro* and *in*
581 *vivo* maintained juvenile fluke relate to their divergent growth rate/stem cell proliferation and
582 the developmental differences seen in the two groups of parasites. The data expose a key

583 role for miRNAs in coordinating the developmental differences seen in *in vivo* (fast growing)
584 and *in vitro* (slow growing) juveniles. Further, the data highlight dramatic changes in the
585 expression of neuronal signalling systems, consistent with a role for the nervous system in
586 suppressing the growth and development of *F. hepatica* juveniles. The observations
587 encourage the search for new potential control targets associated with signalling systems that
588 regulate juvenile growth/development in liver fluke.

589

590 **Materials and Methods**

591 *Ethical statement*

592 This work was carried out in accordance with the Animals (Scientific Procedures) Act 1986
593 adopting the principles of the 3Rs (Replacement, Reduction and Refinement). The Animal
594 Project Licence was: PPL 2764. The methods proposed under the licence were approved by
595 the QUB Animal Welfare Ethical Review Body and animals were euthanised using carbon
596 dioxide gas.

597

598 *Fasciola hepatica material*

599 Italian strain *F. hepatica* metacercariae were purchased from Ridgeway Research for
600 generation of transcriptomes. For *in vivo* maintained *F. hepatica*, 16 Sprague-Dawley rats
601 were infected with 25 metacercariae each and maintained for 21 days before fluke were
602 recovered from liver tissue. Livers were cubed and incubated at 37°C, 5% CO_2 to allow
603 juvenile fluke to emerge for collection. All juveniles were collected within 2 hours of initial liver
604 processing, washed five times in RPMI to remove liver material and snap frozen for storage
605 at -80°C prior to further processing. One biological replicate contained 9 juveniles from at
606 least 3 rats. *In vitro* maintained juvenile replicates were manually excysted as described by
607 McVeigh et al. with a prior preparation step of removing the outer casing of metacercariae and

608 bleaching for 2-3 minutes [85]. Excystments of replicates were carried out on consecutive
609 days to generate a total of 1000 juveniles per replicate. Juveniles were maintained in 50%
610 chicken serum and RPMI as described by McCusker *et al.* for 21 days prior to being snap
611 frozen for storage at -80°C prior to further processing [15]. Juveniles maintained under
612 anaerobic conditions were placed in an anaerobic chamber (Don Whitley Scientific, Shipley,
613 UK) set to 37°C and supplied with anaerobic mixed gas (10% CO2, 10% H2 in N2, BOC). To
614 facilitate the maintenance of anaerobic conditions, media were incubated under anaerobic
615 conditions for at least 4 h prior to media changes which were carried out daily. A time-matched
616 control group was maintained as standard with 5% CO2. The pH of anaerobic media was
617 checked to ensure that increased CO2 levels did not render it significantly more acidic than
618 media incubated at 5% CO2. Trials ran for a duration of 3 weeks, with worm survival being
619 monitored on a weekly basis. Worm death was defined by a total lack of movement and
620 darkened appearance.

621

622 *Labelling proliferative nuclei with 5-ethynyl-2-deoxyuridine (EdU)*

623 Visualisation of *Fasciola* proliferative cells from 21 day old juveniles maintained *in vitro* and *in*
624 *vivo* was achieved by labelling nuclei undergoing DNA-synthesis with 5-ethynyl-2-
625 deoxyuridine (EdU; ThermoFisher Scientific) as described by [15]. Incubations were carried
626 out at a final concentration of 500 µM in 50% chicken serum for 24 hours. Juveniles were
627 then flat fixed in 4% paraformaldehyde under coverslips for 10 minutes (*in vitro*) and 40
628 minutes (*in vivo*) followed by 4-hours free-fixing at room temperature. EdU incubated, fixed
629 juveniles were processed for detection using the Click-iT EdU Alexa Fluor 488 imaging kit, as
630 per kit instructions (ThermoFisher Scientific). Background labelling of all nuclear DNA was
631 achieved using 4′,6-diamidino-2-phenylindole (DAPI). Samples for analysis were mounted in
632 Vectasheild (Vector Laboratories) and viewed on Leica TCS SP5 or SP8 confocal
633 microscopes as maximally projected z-stacks generated from 12-15 optical sections from
634 ventral to dorsal surface.

635

636 *RNA extraction, library preparation and sequencing*

637 3 biological replicates of *in vitro* maintained and *in vivo* retrieved juveniles were prepared.
638 RNA was extracted using TRIzol reagent (Life Technologies) with an isopropanol precipitation,
639 using glycogen as a carrier. Precipitation was performed overnight at -20°C to maximise small
640 RNA recovery. RNA was DNase treated using the Turbo DNase kit (Ambion) following
641 manufacturer's instructions and quality control was performed using bioanalyzers to assess
642 for degradation; Qubit for accurate quantification and NanoDrop to indicate sample purity. All
643 accepted samples displayed a 260/280 >2, *i.e*. pure RNA with no protein contamination, and
644 a 260/230 >1.8. Sample library preparation and sequencing were carried out by the Centre
645 for Genomic Research at the University of Liverpool as follows. For RNAseq, libraries were
646 prepared using a PolyA selection and the NEBNext Ultra Directional RNA library kit for Illumina
647 to prepare dual indexed, strand specific libraries. Paired end sequencing (2x150bp) was
648 performed on the 6 libraries (3 *in vivo*, 3 *in vitro*) using the Illumina HiSeq 4000 platform and
649 generated in excess of 280M mappable reads (~47M reads per sample). For small-RNAseq,
650 libraries were prepared using the NEBNext Small RNA library preparation kit for Illumina and
651 single-end sequencing (1x50bp) performed on the HiSeq2500 platform.

652

653 *Assembly, annotation and sequence data analyses*

654 Raw sequences were trimmed for the presence of Illumina adapter sequences using Cutadapt
655 (v.1.2.1) [86] and low quality reads using Sickle (v.1.200) [87] with a minimum window quality
656 score of 20. Remaining reads under 10bp were removed. Final quality control was performed
657 using FastQC (v.0.11.8) [88] with default parameters. The *F. hepatica* genome contigs
658 (PRJEB25283) and associated GFF file (PRJEB25283) were downloaded from WormBase
659 ParaSite (WBPS14; https://parasite.wormbase.org/index.html) [89] and annotations were
660 converted to GTF format using Cufflink (v.2.2.2.20150701) [90]. Trimmed FastQT files were

661 aligned to the *F hepatica* genome (PRJEB25283) using HISAT2 (v.2.1.0) [91] with default
662 parameters and transcripts compiled and counted using StringTie (v.1.3.6) [92, 93].
663 Annotated transcripts were combined to generate a gene count file, removing transcript
664 isoforms. Gene count datasets were filtered to remove non-coding genes and reads with zero
665 gene counts. Data were normalised for sequencing depth and RNA composition using
666 DESeq2 (v.1.26.0) [94] package in R (v.3.6.2) [95] with default parameters.

667

668 *Annotation and analysis of genes of interest*

669 Raw gene count datasets generated as previously described were mined for genes absent in
670 one treatment group (across 3 replicates of *in vitro* or *in vivo* transcriptomes) and present in
671 at least 2 replicates of the opposite treatment group with a total gene count ≥10. These genes
672 were designated as switched 'on' or 'off' *in vivo*. Differential expression analysis of protein
673 coding genes was quantified using the DESeq2 (v.1.14.1) [84, 96] package in R (v.3.6.2) [95].
674 A p-value threshold was set for a false discovery rate (FDR) of <0.001 and no threshold was
675 applied for fold change differences. Genes identified using these parameters were described
676 as upregulated or downregulated *in vivo*. Differentially expressed genes were annotated as
677 described in Fig 1. BLASTx analysis of gene sequences was carried out against the NCBI
678 non-redundant protein (nr) database. Transdecoder (v.5.5.0) was used to identify candidate
679 open reading frames and translate genes to proteins for BLASTp analysis against Uniprot
680 reviewed sequence database. Top hit annotations were collated from both BLAST databases
681 with a p-value ≤0.05. Domain analysis was carried out on predicted proteins using
682 Interproscan (v.5.36-75.0) and PFAM domain analysis using hmmscan functions of HMMER
683 (v.3.1) (p-value ≤0.05). Differentially expressed genes also underwent KEGG pathway
684 analysis to identify important biological pathway differences within datasets. BlastKOALA was
685 used to assign KEGG gene K numbers based on matches with known human pathway genes.
686 R (v.3.6.2) packages DESeq2 (v.1.26.0), gage (v.2.36.0) and pathview (v.1.26.0) were used

687 to analyse results using custom R scripts and determine significant differences (p-value
688 ≤0.05). GO term analysis was also carried out on genes annotated in the *F. hepatica* genome
689 using data retrieved from WormBase ParaSite (WBPS14;
690 https://parasite.wormbase.org/index.html) [89]. Data were visualised using GraphPad Prism
691 (v.8) and R (v.3.6.2) packages DESeq2 (v.1.26.0), ggplot2 (v.3.3.1) and upsetR. (v.1.4.0) with
692 custom R scripts.

693

694 *Identification and differential expression analysis of miRNAs in in vivo and in vitro maintained*
695 *F. hepatica*

696 Small RNA fastq files were aligned to a Bowtie index of *F. hepatica* genome PRJEB25283
697 using miRDeep2 (v 2.0.1.2) [97]. miRNAs were defined using the following criteria; present in
698 at least 2 out of 3 replicates for either *in vitro* or *in vivo* transcriptomes, a minimum of 10 reads
699 mapped to the mature sequence, at least 1 read mapped to the star sequence, a significant
700 randfold value and a minimum miRDeep2 score of 5. miRNA naming was consistent with that
701 presented in Herron et al. [49]. Differential expression of identified miRNAs was carried out
702 using DESeq2 (version 1.28.1), with an adjusted *p*-value of 0.001 for significance. miRNA
703 target prediction was then carried out using miRanda (version 3.3) [98], with thresholds of
704 minimum pairing score of 150 and maximum free energy score of -20. Predicted targets were
705 refined to those differentially expressed in *in vitro* and *in vivo* mRNA transcriptomes and
706 correlating with miRNA expression, i.e. upregulated in *in vivo* miRNA datasets and
707 downregulated in *in vivo* mRNA datasets, for further interpretation. GO terms associated with
708 predicted miRNA targets were retrieved from WormBase ParaSite (WBPS15) and manually
709 interpreted for frequency (number of times GO term was present in datasets) plotted against
710 Log2 fold change from previous transcriptome analysis.

711

712 **Acknowledgements**

713 The authors acknowledge the National Centre for the Replacement, Refinement and
714 Reduction of Animals in Research (NC3Rs) grant NC/N001486/1, the Biotechnology and
715 Biological Sciences Research Council (BBSRC) grant BB/T002727/1 and The Department for
716 Education (DfE) and the Department for Agriculture, Environment and Rural Affairs (DAERA)
717 for postgraduate studentship support for DW, EG, NC and RA.

718

719

720 **References**

721 1. World Health Organisation. The “Neglected” Neglected Worms. Action Against Worms.
722 2007. Available from: https://www.who.int/publications/i/item/WHO-HTM-NTD-NZD-
723 2008.2.
724 2. Spithill T, Smooker P, Coperman D. Fasciola gigantica: epidemiology, control,
725 immunology and molecular biology. In: Dalton J, ed. by. Fasciolosis. 1st ed. Oxworth:
726 Commonwealth Agricultural Bureau International; 1999. p. 465-525.
727 3. Webb C, Cabada M. Recent developments in the epidemiology, diagnosis, and
728 treatment of Fasciola infection. Current Opinion in Infectious Diseases.
729 2018;31(5):409-414. PMID: 30113327.
730 4. Fairweather I, Brennan G, Hanna R, Robinson M, Skuce P. Drug resistance in liver
731 flukes. International Journal for Parasitology: Drugs and Drug Resistance. 2020;12:39-
732 59. PMID: 32179499.
733 5. Tolan Jr RW. Fascioliasis due to Fasciola hepatica and Fasciola gigantica infection:
734 an update on this ‘neglected’ neglected tropical disease. Laboratory Medicine. 2011
735 Feb 1;42(2):107-16.
736 6. Kelley J, Elliott T, Beddoe T, Anderson G, Skuce P, Spithill T. Current Threat of
737 Triclabendazole Resistance in Fasciola hepatica. Trends in Parasitology.
738 2016;32(6):458-469. PMID: 27049013.
739 7. Kaplan R. Fasciola hepatica: a review of the economic impact in cattle and
740 considerations for control. Veterinary Therapeutics. 2001;2(1):40-50.
741 8. Cwiklinski K, Jewhurst H, McVeigh P, Barbour T, Maule A, Tort J et al. Infection by the
742 Helminth Parasite Fasciola hepatica Requires Rapid Regulation of Metabolic,
743 Virulence, and Invasive Factors to Adjust to Its Mammalian Host. Molecular & Cellular
744 Proteomics. 2018;17(4):792-809. PMID: 29321187.
745 9. John B, Davies D, Williams D, Hodgkinson J. A review of our current understanding of
746 parasite survival in silage and stored forages, with a focus onFasciola

747 hepaticametacercariae. Grass and Forage Science. 2019;74(2):211-217. PMID:
748 31244499.
749 10. Gajewska A, Smaga-Kozłowska K, Wiśniewski M. Pathological changes of liver in
750 infection of Fasciola hepatica. Wiad Parazytol. 2005;51(2):115-123. PMID: 16838620.
751 11. Di Maggio L, Tirloni L, Pinto A, Diedrich J, Yates III J, Benavides U et al. Across intra-
752 mammalian stages of the liver fluke Fasciola hepatica: a proteomic study. Scientific
753 Reports. 2016;6(1). PMID: 27600774.
754 12. Gil L, Díaz A, Rueda C, Martínez C, Castillo D, Apt W. Fascioliasis hepática humana:
755 resistencia al tratamiento con triclabendazol. Revista médica de Chile.
756 2014;142(10):1330-1333. PMID: 25601119.
757 13. Cabada M, Lopez M, Cruz M, Delgado J, Hill V, White A. Treatment Failure after
758 Multiple Courses of Triclabendazole among Patients with Fascioliasis in Cusco, Peru:
759 A Case Series. PLOS Neglected Tropical Diseases. 2016;10(1):e0004361. PMID:
760 26808543.
761 14. Branco E, Ruas R, Nuak J, Sarmento A. Treatment failure after multiple courses of
762 triclabendazole in a Portuguese patient with fascioliasis. BMJ Case Reports.
763 2020;13(3):e232299. PMID: 32193176.
764 15. McCusker P, McVeigh P, Rathinasamy V, Toet H, McCammick E, O'Connor A et al.
765 Stimulating Neoblast-Like Cell Proliferation in Juvenile Fasciola hepatica Supports
766 Growth and Progression towards the Adult Phenotype In Vitro. PLOS Neglected
767 Tropical Diseases. 2016;10(9):e0004994. PMID: 27622752.
768 16. Duque-Correa M, Maizels R, Grencis R, Berriman M. Organoids – New Models for
769 Host–Helminth Interactions. Trends in Parasitology. 2020;36(2):170-181. PMID:
770 31791691.
771 17. Wang J, Chen R, Collins J. Systematically improved in vitro culture conditions reveal
772 new insights into the reproductive biology of the human parasite Schistosoma
773 mansoni. PLOS Biology. 2019;17(5):e3000254. PMID: 31067225.
774

775 18. McVeigh P, McCusker P, Robb E, Wells D, Gardiner E, Mousley A et al. Reasons to
776 Be Nervous about Flukicide Discovery. Trends in Parasitology. 2018;34(3):184-
777 196.PMID: 29269027
778 19. Young ND, Hall RS, Jex AR, Cantecessi C, Gasser RB. Elucidating the transcriptome
779 of Fasciola hepatica - a key to fundamental and biotechnological discoveries for a
780 neglected parasite. 2010;28(2):222-231. PMID: 20006979
781 20. Cwiklinski K, Dalton J, Dufresne P, La Course J, Williams D, Hodgkinson J et al. The
782 Fasciola hepatica genome: gene duplication and polymorphism reveals adaptation to
783 the host environment and the capacity for rapid evolution. Genome Biology.
784 2015;16(1). PMID: 25887684.
785 21. Radio S, Fontenla S, Solana V, Matos Salim A, Araújo F, Ortiz P et al. Pleiotropic
786 alterations in gene expression in Latin American Fasciola hepatica isolates with
787 different susceptibility to drugs. Parasites & Vectors. 2018;11(1). PMID: 29368659.
788 22. Cwiklinski K, Robinson MW, Donnelly S, Dalton JP. Complementary transcriptomic and
789 proteomic analyses reveal the cellular and molecular processes that drive growth and
790 development of Fasciola hepatica in the host liver. BMC Genomics. 2021;22(1). PMID:
791 33430759.
792 23. Miranda-Miranda E, Cossio-Bayugar R, Aguilar- Díaz H, Narváez-Padilla V, Sachman-
793 Ruíz B, Reynaud E. Transcriptome assembly dataset of anthelmintic response in
794 Fasciola hepatica. Data in Brief. 2021;35:106808. PMID: 33659584.
795 24. Collins III J, Wang B, Lambrus B, Tharp M, Iyer H, Newmark P. Adult somatic stem
796 cells in the human parasite Schistosoma mansoni. Nature. 2013;494(7438):476-479.
797 PMID: 23426263.
798 25. Giri B, Li H, Chen Y, Cheng G. Preliminary evaluation of neoblast-like stem cell factor
799 and transcript expression profiles in Schistosoma japonicum. Acta Tropica.
800 2018;187:57-64. PMID: 30055172.

801 26. Cwiklinski K, Donnelly S, Drysdale O, Jewhurst H, Smith D, De Marco Verissimo C et
802 al. The cathepsin-like cysteine peptidases of trematodes of the genus Fasciola.
803 Advances in Parasitology. 2019;:113-164. PMID: 31030768.
804 27. Dalton J, Neill S, Stack C, Collins P, Walshe A, Sekiya M et al. Fasciola hepatica
805 cathepsin L-like proteases: biology, function, and potential in the development of first
806 generation liver fluke vaccines. International Journal for Parasitology.
807 2003;33(11):1173-1181. PMID: 13678633.
808 28. Robinson M, Menon R, Donnelly S, Dalton J, Ranganathan S. An Integrated
809 Transcriptomics and Proteomics Analysis of the Secretome of the Helminth Pathogen
810 Fasciola hepatica. Molecular & Cellular Proteomics. 2009;8(8):1891-1907. PMID:
811 19443417.
812 29. Grote A, Caffrey C, Rebello K, Smith D, Dalton J, Lustigman S. Cysteine proteases
813 during larval migration and development of helminths in their final host. PLOS
814 Neglected Tropical Diseases. 2018;12(8):e0005919. PMID: 30138448.
815 30. Wang Q, Da'dara A, Skelly P. The human blood parasite Schistosoma mansoni
816 expresses extracellular tegumental calpains that cleave the blood clotting protein
817 fibronectin. Scientific Reports. 2017;7(1). PMID: 29018227.
818 31. Tielens A, van Hellemond J. Unusual aspects of metabolism. In: Maule A, Marks N,
819 ed. by. Parasitic flatworms: molecular biology, biochemistry, immunology and
820 physiology. CAB International; 2006. p. 387-408.
821 32. McVeigh P, Cwiklinski K, Garcia-Campos A, Mulcahy G, O'Neill S, Maule A et al. In
822 silico analyses of protein glycosylating genes in the helminth Fasciola hepatica (liver
823 fluke) predict protein-linked glycan simplicity and reveal temporally-dynamic
824 expression profiles. Scientific Reports. 2018;8(1).
825 33. Harada Y, Ohkawa Y, Kizuka Y, Taniguchi N. Oligosaccharyltransferase: A
826 Gatekeeper of Health and Tumor Progression. International Journal of Molecular
827 Sciences. 2019;20(23):6074. PMID: 31810196.

828 34. Hokke C, van Diepen A. Helminth glycomics – glycan repertoires and host-parasite
829 interactions. Molecular and Biochemical Parasitology. 2017;215:47-57. PMID:
830 27939587.
831 35. 13. Lin B, Qing X, Liao J, Zhuo K. Role of Protein Glycosylation in Host-Pathogen
832 Interaction. Cells. 2020;9(4):1022. PMID: 32326128.
833 36. Davis R, Stretton A. Neurotransmitters of Helminths. In: Marr J, Müller M, ed. by.
834 Biochemistry and Molecular Biology of Parasites. Elsevier; 1995.
835 37. McVeigh P, Kimber M, Novozhilova E, Day T. Neuropeptide signalling systems in
836 flatworms. Parasitology. 2006;131(S1):S41. PMID: 16569292.
837 38. McVeigh P, Maule A. Flatworm Neurobiology in the Postgenomic Era. In: Byrne JH,
838 ed. by. The Oxford Handbook of Invertebrate Neurobiology. Oxford University Press;
839 2017.
840 39. Südhof TC. The synaptic vesicle cycle: a cascade of protein-protein interactions.
841 Nature. 1995;375(6533):645-53. PMID: 7791897.
842 40. Ribeiro P, El-Shehabi F, Patocka N. Classical transmitters and their receptors in
843 flatworms. Parasitology. 2005;S131:S19-40. PMID: 16569290.
844 41. Fairweather I, Maule A, Mitchell S, Johnston C, Halton D. *I*mmunocytochemical
845 demonstration of 5-hydroxytryptamine (serotonin) in the nervous system of the liver
846 fluke, Fasciola hepatica (Trematoda, Digenea). Parasitology Research. 1987;**73**(3):
847 255-8. PMID: 3295862.
848 42. Tembe E, Holden-Dye L, Smith S, Jacques P, Walker R. Pharmacological profile of
849 the 5-hydroxytryptamine receptor of Fasciola hepatica body wall muscle. Parasitology.
850 1993;106(Pt1):67-73. PMID: 8479803.
851 43. McVeigh P, Mair G, Atkinson L, Ladurner P, Zamanian M, Novozhilova E, Marks N,
852 Day T, Maule A. Discovery of multiple neuropeptide families in the phylum
853 Platyhelminthes. International Journal for Parasitology. 2009;**39**(11):1243-52. PMID:
854 19361512.

855 44. McVeigh P, McCammick E, McCusker P, Wells D, Hodgkinson J, Paterson S, Mousley
856 A, Marks N, Maule A. Profiling G protein-coupled receptors of Fasciola hepatica
857 identifies orphan rhodopsins unique to phylum Platyhelminthes. International Journal
858 for Parasitology: Drugs and Drug Resistance. 2018;8(1):87-103. PMID: 29474932
859 45. Xu M, Ai L, Fu J, Nisbet A, Liu Q, Chen M et al. Comparative Characterization of
860 MicroRNAs from the Liver Flukes Fasciola gigantica and F. hepatica. PLoS ONE.
861 2012;7(12):e53387. PMID: 23300925.
862 46. Fromm B, Trelis M, Hackenberg M, Cantalapiedra F, Bernal D, Marcilla A. The revised
863 microRNA complement of Fasciola hepatica reveals a plethora of overlooked
864 microRNAs and evidence for enrichment of immuno-regulatory microRNAs in
865 extracellular vesicles. International Journal for Parasitology. 2015;45(11):697-702.
866 PMID: 26183562
867 47. Fontenla S, Dell'Oca N, Smircich P, Tort J, Siles-Lucas M. The miRnome of Fasciola
868 hepatica juveniles endorses the existence of a reduced set of highly divergent micro
869 RNAs in parasitic flatworms. International Journal for Parasitology. 2015;45(14):901-
870 913. PMID: 26432296.
871 48. Ovchinnikov V, Kashina E, Mordvinov V, Fromm B. EV-transported microRNAs of
872 Schistosoma mansoni and Fasciola hepatica: Potential targets in definitive hosts.
873 Infection, Genetics and Evolution. 2020;85:104528.
874 49. Herron C, O'Connor A, Robb E, McCammick E, Hill C, Marks N et al. Developmental
875 regulation and functional prediction of microRNAs in an expanded Fasciola hepatica
876 miRNome. 2021;.
877 50. Kaltz O, Shykoff JA. Local adaptation in host-parasite systems. Heredity.
878 1998;81(4):361-370.
879 51. Read AF, Skorping A. The evolution of tissue migration by parasitic nematode larvae.
880 Parasitology. 1995;111(Pt 3):359-71. PMID: 7567104.

881 52. Orrego-Solano MA, Cangalaya C, Nash T, Guerra-Giraldez C, de Trabajo en
882 Cisticercosis en Peru. Identification of proliferating cells in Taenia solium cyst. Rev
883 Peru Med Exp Salud Publica. 2014;**31**(4):702-6. PMID: 25597721
884 53. Baguñà J. The planarian neoblast: the rambling history of its origin and some current
885 black boxes. The International Journal for Developmental Biology. 2012;56(1-3):19-
886 37. PMID: 22252540.
887 54. Rink JC. Stem cell systems and regeneration in planaria. Developmental Genes and
888 Evolution. 2013;223(1-2):67-84. PMID: 23138344.
889 55. Koziol U, Rauschendorfer T, Rodríguez LZ, Krohne G, Brehm K. The unique stem cell
890 system of the immortal larva of the human parasite Echinococcus multilocularis.
891 Evodevo. 2014;**5**(1):10. PMID: 24602211.
892 56. Collins JJ, Wendt GR, Lyer H, Newmark PA. Stem cell progeny contribute to the
893 schistosome host-parasite interface. Elife. 2016;**5**:e12473. PMID: 27003592.
894 57. Collins JN, Collins JJ. Tissue Degeneration following Loss of Schistosoma mansoni
895 cbp1 Is Associated with Increased Stem Cell Proliferation and Parasite Death In Vivo.
896 PLoS Pathogen. 2016;**12**(11):e1005963. PMID: 27812220
897 58. Akiba Y, Chida Y, Takahashi T, Ohtomo Y, Sato K, Takahashi K. Persistent
898 hypoglycemia induced by continuous insulin infusion in broiler chickens. British Poultry
899 Science. 1999;**40**(5):701-5. PMID: 10670686
900 59. Tielens AG, van den Heuvel JM, van den Bergh. The energy metabolism of Fasciola
901 hepatica during its development in the final host. Molecular and Biochemical
902 Parasitology. 1984;13(3):301-307. PMID: 6527693
903 60. Alvarado R, To J, Lund ME, Pinar A, Mansell A, Robinson MW, O'Brien BA, Dalton JP,
904 Donnelly S. The immune modulatory peptide FhHDM-1 secreted by the helminth
905 Fasciola hepatica prevents NLRP3 inflammasome activation by inhibiting
906 endolysosomal acidification in macrophages. The FASEB Journal. 2017;31(1):85-95.
907 PMID: 27682204.

908 61. Martínez-Sernández V, Mezo M, González-Warleta M, Perteguer MJ, Muiño L, Guitián
909 E, Gárate T, Ubeira FM. The MF6p/FhHDM-1 major antigen secreted by the trematode
910 parasite Fasciola hepatica is a heme-binding protein. Journal of Biological Chemistry.
911 2014;289(3):1441-56. PMID: 24280214.
912 62. Robinson M, Donnelly S, Dalton JP. Helminth defence molecules-immunomodulators
913 designed by parasites! Frontiers in Microbiology. 2013;**4**:296. PMID: 24101918
914 63. Freeze HH, Elbein AD. Glycosylation precursors. In: Varki A, Cummings RD, Esko JD,
915 Stanley P, Hart GW, Aebi M, Darvill AG, Kinoshita T, Packer NH, Prestegard JH,
916 Schnaar RL, Seeberger PH. ed. by. Essentials of Glycobiology. 2009. Cold Spring
917 Harbor Laboratory Press.
918 64. Fadda M, Hasakiogullari I, Temmerman L, Beets I, Zels S, Schoofs L. Regulation of
919 Feeding and Metabolism by Neuropeptide F and Short Neuropeptide F in
920 Invertebrates. Frontiers in Endocrinology. 2019;**10**(64). PMID: 30837946.
921 65. Camacho M, Agnew A. Schistosoma: rate of glucose import is altered by acetylcholine
922 interaction with tegumental acetylcholine receptors and acetylcholinesterase.
923 Experimental Parasitology. 1995;81(4):584-91. PMID: 8543000.
924 66. Nässel DR, Wegener C. A comparative review of short and long neuropeptide F
925 signaling in invertebrates: Any similarities to vertebrate neuropeptide Y signaling?
926 Peptides. 2011;**32**(6):1335-55. PMID: 21440021.
927 67. Wu Q, Zhao Z, Shen P. Regulation of aversion to noxious food by Drosophila
928 neuropeptide Y- and insulin-like systems. Nature Neuroscience. 2005;8(10):1350-5.
929 PMID: 16172603.
930 68. Chen J, Cheuk I, Shin V, Kwong A. Acetylcholine receptors: Key players in cancer
931 development. Surgical Oncology. 2019;31:46-53. PMID: 31536927
932 69. Weist R, Flörkemeier T, Roger Y, Franke A, Schwanke K, Zweigerdt R, Martin U,
933 Willbold E, Hoffman A. Differential Expression of Cholinergic System Components in
934 Human Induced Pluripotent Stem Cells, Bone Marrow-Derived Multipotent Stromal

935 Cell, and Induced Pluripotent Stem Cell-Derived Multipotent Stromal Cells. Stem Cells
936 and Development. 2018;27(3):166-183. PMID: 29205106.
937 70. Landgraf D, Barth M, Layer PG, Sperling LE. Acetylcholine as a possible signaling
938 molecule in embryonic stem cells: studies on survival, proliferation and death.
939 Chemico-Biological Interactions. 2010. **187**(1-3): p. 115-119. PMID: 20223227.
940 71. Gingle AR. Acetylcholine and carnitine sensitive growth in a Drosophila cell line.
941 Comparative Biochemistry Physiology Part C: Pharmacology and Toxicology.
942 1985;82(1): p. 235-41. PMID: 2865070.
943 72. Ruaud AF, Bessereau JL. The P-type ATPase CATP-1 is a novel regulator of C.
944 elegans developmental timing that acts independently of its predicted pump function.
945 Development. 2007;134(5):867-79. PMID: 17251264.
946 73. Li BW, Rush AC, Weil GJ. Expression of five acetylcholine receptor subunit genes in
947 Brugia malayi adult worms. International Journal for Parasitology: Drugs Drug
948 Resistance. 2015;5(3):100-9. PMID: 26199859.
949 74. Kreshchenko ND, Functions of flatworm neuropeptides NPF, GYIRF and FMRF in
950 course of pharyngeal regeneration of anterior body fragments of planarian, Girardia
951 tigrina. Acta Biologica Hungarica. 2008; 59:199-207. PMID: 18652393.
952 75. Collins JJ, Hou X, Romanova EV, Lambrus BG, Miller CM, Saberi A, Sweedler JV,
953 Newmark PA. Genome-wide analyses reveal a role for peptide hormones in planarian
954 germline development. PLoS Biology. 2010;8(10):1000509. PMID: 20967238.
955 76. Ameku T, Yoshino Y, Texada MJ, Kondo S, Amezawa, Yoshizaki G, Shimida-Niwa Y,
956 Niwa R. Midgut-derived neuropeptide F controls germline stem cell proliferation in a
957 mating-dependent manner. PLoS Biology. 2018;16(9):e2005004. PMID: 30248087.
958 77. Wang B, Collins JJ, Newmark PA. Functional genomic characterization of neoblast-
959 like stem cells in larval Schistosoma mansoni. Elife. 2013;2:e00768. PMID: 23908765.
960 78. Saberi A, Jamal A, Beets I, Schoofs L, Newmark P. GPCRs Direct Germline
961 Development and Somatic Gonad Function in Planarians. PLOS Biology.
962 2016;14(5):e1002457.PMID: 27163480.

963 79. Shivdasani R. MicroRNAs: regulators of gene expression and cell differentiation.
964 Blood. 2006;108(12):3646-3653.PMID: 16882713.
965 80. Worringer K, Rand T, Hayashi Y, Sami S, Takahashi K, Tanabe K et al. The let-7/LIN-
966 41 Pathway Regulates Reprogramming to Human Induced Pluripotent Stem Cells by
967 Controlling Expression of Prodifferentiation Genes. Cell Stem Cell. 2014;14(1):40-
968 52.PMID: 24239284.
969 81. Hunter S, Finnegan E, Zisoulis D, Lovci M, Melnik-Martinez K, Yeo G et al. Functional
970 Genomic Analysis of the let-7 Regulatory Network in Caenorhabditis elegans. PLoS
971 Genetics. 2013;9(3):e1003353.PMID: 23516374.
972 82. Makeyev E, Zhang J, Carrasco M, Maniatis T. The MicroRNA miR-124 Promotes
973 Neuronal Differentiation by Triggering Brain-Specific Alternative Pre-mRNA Splicing.
974 Molecular Cell. 2007;27(3):435-448.PMID: 17679093.
975 83. Li K, Pang J, Ching A, Wong C, Kong X, Wang Y et al. miR-124 is frequently down-
976 regulated in medulloblastoma and is a negative regulator of SLC16A1. Human
977 Pathology. 2009;40(9):1234-1243.PMID: 19427019.
978 84. Song J, Nigam P, Tektas S, Selva E. microRNA regulation of Wnt signaling pathways
979 in development and disease. Cellular Signalling. 2015;27(7):1380-1391.
980 85. McVeigh P, McCammick E, McCusker P, Morphew R, Mousley A, Abidi A et al. RNAi
981 Dynamics in Juvenile Fasciola spp. Liver Flukes Reveals the Persistence of Gene
982 Silencing In Vitro. PLoS Neglected Tropical Diseases. 2014;8(9):e3185. PMID:
983 25254508.
984 86. Martin M. Cutadapt removes adapter sequences from high-throughput sequencing
985 reads. EMBnetjournal. 2011;17(1):10.
986 87. 4. Joshi N. Sickle: A sliding-window, adaptive, quality-based trimming tool for FastQ
987 files (version 1.33). 2011. Available from: https://github.com/najoshi/sickle.
988 88. Andrews S. FastQC: A quality control tool for high throughput sequence data. 2010.
989 Available from: http://www.bioinformatics.babraham.ac.uk/projects/fastqc/.

89. Howe K, Bolt B, Shafie M, Kersey P, Berriman M. WormBase ParaSite − a comprehensive resource for helminth genomics. Molecular and Biochemical Parasitology. 2017;215:2-10. PMCID: PMC5486357.

90. Trapnell C, Williams B, Pertea G, Mortazavi A, Kwan G, van Baren M et al. Transcript assembly and quantification by RNA-Seq reveals unannotated transcripts and isoform switching during cell differentiation. Nature Biotechnology. 2010;28(5):511-515. PMID: 20436464.

91. Kim D, Langmead B, Salzberg S. HISAT: a fast spliced aligner with low memory requirements. Nature Methods. 2015;12(4):357-360. PMID: 25751142.

92. Pertea M, Pertea G, Antonescu C, Chang T, Mendell J, Salzberg S. StringTie enables improved reconstruction of a transcriptome from RNA-seq reads. Nature Biotechnology. 2015;33(3):290-295. PMID: 25690850.

93. Pertea M, Kim D, Pertea G, Leek J, Salzberg S. Transcript-level expression analysis of RNA-seq experiments with HISAT, StringTie and Ballgown. Nature Protocols. 2016;11(9):1650-1667. PMID: 27560171.

94. Love M, Huber W, Anders S. Moderated estimation of fold change and dispersion for RNA-seq data with DESeq2. Genome Biology. 2014;15(12). PMID: 25516281.

95. R Core Team. R: A language and environment for statistical computing. R Foundation for Statistical Computing, Vienna, Austria. 2018. Available from: http://www.R-project.org.

96. Love MI, Anders S, Huber W. Analyzing RNA-seq data with DESeq2. 2020. Available from: http://bioconductor.org/packages/devel/bioc/vignettes/DESeq2/inst/doc/DESeq2.html

97. Friedländer M, Mackowiak S, Li N, Chen W, Rajewsky N. miRDeep2 accurately identifies known and hundreds of novel microRNA genes in seven animal clades. Nucleic Acids Research. 2011;40(1):37-52.PMID: 21911355.

98. Betel D, Koppal A, Agius P, Sander C, Leslie C. Comprehensive modeling of microRNA targets predicts functional non-conserved and non-canonical sites. Genome Biology. 2010;11(8):R90.PMID: 20799968.

Fig 1: Flow chart of bioinformatics pipeline. Outline of methods used to assemble and analyse transcriptomes. Low quality reads and adapters were removed using Cutadapt (v.1.2.1) and Sickle (v.1.200) and remaining reads quality assessed using FastQC (v. 0.11.8) analysis. High quality reads were aligned to the *Fasciola hepatica* transcriptome (PRJEB25283) using HISAT2 (v.2.1.0) and transcripts generated from genome annotation (PRJEB25283) and counted using StringTie (v.1.3.6). Raw gene counts were reviewed for genes of interest (GOI) and analysed for differential expression using R version 3.6.2 and DESeq2 (v.1.26.0) package (FDR <0.001). A core annotation pipeline was developed to annotate GOI's using BLASTx against NCBI non redundant protein (nr) database; predicted proteins generated using Transdecoder; BLASTp predicted proteins against uniprot reviewed sequence database; functional domain analysis interrogating PFAM and interproscan databases. Graphs were visualised using ggplot2, gate, pathview and upsetR R packages using custom scripts. Chart generated online at: https://app.lucidchart.com. Abbreviations; ivt=*in vitro*, ivv=*in vivo.*

Fig 2: *In vitro* and *in vivo* maintained juvenile liver fluke display differences in growth and cell proliferation rate. (A) Cell proliferation represented by EdU+ cells (green) of 21 day old (+1 day staining) *in vitro* maintained juvenile *Fasciola hepatica*. (B) Cell proliferation represented by EdU+ cells (green) of 21 day old (+1 day staining) *in vivo* maintained juvenile *F. hepatica*. Confocal Z stack images; green= EdU+; magenta= DAPI; *in vitro* scale bar= 50 μm; *in vivo* scale bar= 100 μm. **(C) Proliferative cell count (EdU+) per mm² between *in vitro* and *in vivo* maintained juveniles.** A ~4-fold higher cell proliferation rate was seen in *in vivo* maintained juveniles. **(D) Volcano plot of differentially expressed transcripts between *in vitro* and *in vivo* maintained juveniles**. Differential expression analysis and plot generated using R version 3.6.2 and DESeq2 (v.1.26.0) package. Analysis identified 1339 transcripts upregulated and 1320 transcripts downregulated *in vivo* compared to *in vitro* maintained juveniles with a false discovery rate (FDR) of P≤0.001. Red =

1053 significantly differentially expressed transcripts. Grey = not differentially expressed
1054 transcripts.

1055

1056 **Fig 3: *In vivo* juvenile fluke display enhanced expression of genes associated with the**
1057 **cell cycle. (A-C) Gene ontology (GO) term analysis of differentially expressed genes.**
1058 Gene counts associated with GO terms of (A) biological processes, (B) molecular function and
1059 (C) cellular components from differentially expressed and annotated genes on WormBase
1060 ParaSite (v.14). Upregulated datasets contain more genes associated with GO terms of cell
1061 cycle processes and DNA replication whilst downregulated datasets contain a greater number
1062 of genes associated with cell signalling and transport GO terms. Red represents the number
1063 of differentially expressed genes upregulated *in vivo*. Blue represents the number of
1064 differentially expressed genes downregulated *in vivo*. **(D) KEGG pathway analysis of**
1065 **differentially expressed genes.** KEGG pathways considered significantly differentially
1066 expressed as determined by statistical analysis using R (v.3.6.2), gage (v.2.36.0) and
1067 pathview (v.1.26.0) packages ($P \leq 0.05$). Dotted line = 0 $\log_2$FC; dots to the right of dotted line
1068 represent pathways upregulated *in vivo* and dots to the left of the dotted line represent
1069 pathways downregulated *in vivo*. Colour = *p* value; size = gene count.

1070

1071 **Fig 4: *In vivo* juvenile liver fluke displayed upregulation in cell cycle associated genes**
1072 **and neoblast-like stem cell markers. (A) Upset plot showing spread of all transcripts**
1073 **across transcriptome replicates.** 19,343 protein coding genes were generated from
1074 transcriptome analysis. 17,166 genes were found in all generated transcriptomes. Genes of
1075 interest (GOI) include 65 genes present only in *in vitro* transcriptomes and 235 genes present
1076 only in *in vivo* datasets. Limit of analysis restricted to those genes present in at least 2
1077 replicates of either transcriptome (i.e. *in vitro* or *in vivo*). **(B) Cell cycle associated genes**
1078 **upregulated *in vivo*.** Schematic showing phases and progression of the cell cycle

(intermediate (G1), synthesis (S), growth (G2) and mitotic (M) phases). Important genes required for each cell phase to function in the human cell cycle and which have homologues in *Fasciola hepatica* that are upregulated *in vivo* are highlighted in red within the cycle. Those genes only present in *in vivo* datasets are marked with an asterisk (*). Key cyclins (in blue circles) and kinases (in purple squares) required for each phase of the cell cycle to progress in the human cell cycle are highlighted. *F. hepatica* homologues which are upregulated *in vivo* are marked with a red arrow. Important genes required for the cell cycle to function and progress are upregulated *in vivo***.** Abbreviations: CDC(-6, -25, -45), cell division cycle; ORC-3, origin recognition complex subunit 3; CDT-1, chromatin licensing and DNA replication factor 1; MCM2-7, mini-chromosome maintenance complex; TOP-2, DNA topoisomerase 2; Pol-α, DNA polymerase alpha; CTF-4, chromosome transmission fidelity 4; CDK(-1, -2, -4, -6), cyclin-dependent kinase; PLK-1, polo-kinase 1. **(C) Neoblast markers upregulated *in vivo.*** Heatmap showing differentially expressed (log_2FC) neoblast markers in *F. hepatica.* Neoblast markers identified as homologues to markers described by Collins *et al.* [24] in *Schistosoma mansoni*. 53/108 neoblast markers identified in *F. hepatica* were upregulated in *in vivo* datasets.

Fig 5: *In vivo* and *in vitro* juvenile liver fluke show divergent expression of proteases and metabolic enzymes. (A) Cathepsin expression profile across newly excysted juvenile (NEJ), 21 day old juvenile (JUV) and adult *Fasciola hepatica* life stages compared to expression in *in vitro* and *in vivo* maintained *F. hepatica* juveniles. Heatmap showing differential expression of cathepsin B (CATB) and cathepsin L (CATL) encoding transcripts in *in vivo* and *in vitro* maintained *F. hepatica* juveniles (log_2FC) and across *F. hepatica* life stage transcriptomes generated by Cwiklinski *et al.* [20] (NEJ, JUV, ADULT; Z score of fragments per kilobase of transcript per million mapped reads, FPKM). Abbreviated gene IDs in brackets refer to genes in S5. Data show clear pattern of upregulation *in vivo* and greater expression in juvenile and adult transcriptomes, whilst downregulated

genes *in vivo* show greater expression in NEJ transcriptome datasets. **(B) Protease/peptidase profiles of *in vitro* and *in vivo* maintained *F. hepatica* juveniles.** Proportion diagram shows greater expression of cathepsin L and metalloproteases in *in vivo* maintained *F. hepatica* juveniles whilst cathepsin B, legumain and calpain proteases show greater expression in *in vitro* maintained *F. hepatica* juveniles. **(C) Downregulation of key enzymes of aerobic and anaerobic carbohydrate metabolism in *in vivo* maintained *F. hepatica* juveniles.** Expression (log2FC) of key enzymes associated with metabolism in *in vivo* maintained *F. hepatica* juveniles. *Fh*-PK=pyruvate kinase and Fh-SD=succinate dehydrogenase are key enzymes of aerobic metabolism via Kreb's cycle; *Fh*-ME-malic enzyme is a key enzyme of aerobic acetate production; *Fh*-PEPCK=phosphoenolpyruvatecarboxykinase, key enzyme of malate dismutation pathway.

Fig 6: Key neuronal signalling pathways are downregulated in fast growing *in vivo* juvenile liver fluke. Components of classical neurotransmission are downregulated in *in vivo* maintained juvenile liver fluke (A). Analysis and diagrams generated using R (v.3.6.2), gage (v.2.36.0) and pathview (v.1.26.0) packages showing differential expression of nervous system components of the synaptic vesicle cycle, cholinergic signalling and glutamatergic signalling. *Fasciola hepatica* homologues of human components enclosed in rectangular boxes. Green=downregulated *in vivo,* red=upregulated *in vivo*, grey=not differentially expressed, X=not present in *F. hepatica* genome (PRJEB25283). Components are well conserved between human and *F. hepatica* species. KEGG pathway analysis identified a significant downregulation of the synaptic vesicle cycle and cholinergic signalling in *in vivo* maintained *F. hepatica* juveniles. Abbreviations: SYT, synaptotagmin; VAMP, vesicle associated membrane protein; Rab3a, ras-related protein; RIM, regulating synaptic membrane exocytosis protein; MUNC(-13, -18), syntaxin binding protein; SNAP25, synaptosome associated protein; VGCC, voltage-gated calcium channel; NSF, N-ethylmaleimide sensitive factor; αSNAP, NSF associated protein; AP2, adaptor related protein

complex 2; ChAT, choline O-acetyltransferase; AChE, acetylcholinesterase; vAChT, vesicular acetylcholine transporter; CHT, high affinity choline transporter; Gi/o, guanine nucleotide-binding protein; mAChR, muscarinic acetylcholine receptor; nAChR, micotinic acetylcholine receptor; GLNT, amino acid transporter; GLS, glutaminase; vGLUT, vesicular glutamate transporter; GRK, G protein-coupled receptor kinase; AC, adenylate cyclase 1; PKA, protein kinase A; EAAT, glial high affinity glutamate transporter; mGluR, muscarinic glutamate receptor; GluCl, glutamate-gated chloride channel; KA, kainate type ionotropic glutamate receptor; NMDA, NMDA type ionotropic glutamate receptor; DELTA, delta type ionotropic glutamate receptor. **Components of neuropeptidergic signalling pathway are downregulated *in vivo* juvenile liver fluke (B).** Heatmap showing differentially expressed genes associated with neuropeptidergic signalling in *Fasciola hepatica.* All components of the neuropeptide processing pathway are downregulated *in vivo*. Our analysis identified 34 neuropeptide-encoding genes in the *Fasciola hepatica* genome (PRJEB25283) of which 17 are downregulated *in vivo* compared to *in vitro* counterparts. Our analysis further identified 44 peptide GPCRs, an additional 9 compared to the analysis carried out by McVeigh el al [44]. nine peptide GPCRs were downregulated *in vivo*, one of which is hypothesized to be an NPY receptor, whilst 4 were upregulated *in vivo*.

Fig 7: Differences in miRNA profiles of *in vitro* and *in vivo* juveniles support their role in liver fluke developmental processes. **(A) Differential expression of micro (mi)RNA sequences in *in vitro* and *in vivo* maintained 21-day old *Fasciola hepatica* juveniles.** Analysis identified 31 differentially expressed miRNAs between treatment groups (false discovery rate; P≤0.001). Red points highlight significantly upregulated miRNAs *in vivo*, whereas blue points highlight significantly downregulated miRNAs *in vivo*. The two most significantly upregulated miRNAs (*fhe-let-7a-5p,* first identified by Fromm et al. [46] and *fhe-novelmir-55-3p*), downregulated miRNAs (*fhe-mir-124-3p*, first identified by Fontenla et al. [47] and *fhe-pubnovelmir-22-3p* first identified by Fromm et al. [46]) and miRNAs identified as

associated with Wnt signaling (*fhe-mir-10-5p*, *fhe-mir-184-5p*, *fhe-mir-190-5p*, *fhe-mir-2b-3p*, *fhe-pubnovelmir-22-3p*, *fhe-pubnovelmiR-23-3p*, *fhe-novelmir-48-3p*, *fhe-novelmir-50-5p* & *fhe-novelmir-28-3p*) are labelled. Analysis carried out using DESeq2 (v.1.26.0). **(B) Gene ontology (GO) terms associated with biological processes of differentially expressed miRNA predicted gene targets.** GO terms retrieved from WormBase ParaSite (WBPS15) for predicted miRNA targets upregulated or downregulated *in vivo*. Number of individual GO terms associated with biological processes (percentage frequency of total GO terms) plotted alongside average Log_2 fold change of predicted transcripts from differential expression analysis of *in vitro* and *in vivo* maintained *F. hepatica* juveniles. Bubble colour = transcript expression (Log_2FC); bubble size= GO term frequency (percentage gene counts).

Supporting information

S1. File. Transcripts for 21 day old juvenile *Fasciola hepatica* (*in vivo* & *in vitro*)

S2. Table. Transcriptome statistics

S3. Table. Annotations for (A) all genes, (B) differentially expressed genes and (C) on/off genes

S4. Table. (A) Neoblast, (B) cathepsin, (C) metabolomic and (D) neuropeptide markers

S5. Fig. (A) Survival of juvenile liver fluke in aerobic and anaerobic conditions. Percentage survival of juvenile liver fluke across 21 day period post excystment incubated under standard 5% CO2 conditions (red line) and in an anaerobic chamber (purple line). Juveniles showed significant and continuing higher rates of death when maintained in anaerobic chamber after 14 days (2-way ANOVA with Šídák's multiple comparisons test; **** P<0.001). **(B) Components of N-glycan biosynthesis and processing pathways downregulated in *in vivo* maintained *F. hepatica* juveniles.** Differential expression (log_2FC) of protein glycosylating genes associated with N-glycan biosynthesis and processing. Genes identified in *F. hepatica* by McVeigh et al. [32] KEGG pathway analysis using R (v.3.6.2), gage (v.2.36.0) and pathview (v.1.26.0) packages identified a significant

1187 downregulation of N glycan biosynthesis in *in vivo* maintained juveniles (P≤0.05).
1188 Abbreviations; ALG N-glycan precursor synthesis- *Fh*-ALG(-3, -9)=dolichyl-P-
1189 Man:Man(5)GlcNAc(2)-PP-dolichol alpha-1,3-mannosyltransferase, *Fh*-ALG5=dolichyl-
1190 phosphate beta-glucosyltransferase, *Fh*-ALG7= UDP-N-acetylglucosamine--dolichyl-
1191 phosphate N-acetylglucosaminephosphotransferase; Oligosaccharyltransferase complex
1192 components- OST48= dolichyl-diphosphooligosaccharide--protein glycosyltransferase
1193 subunit, *Fh*-RPN(-1, -2)&Fh-STT3(-A, -B)= dolichyl-diphosphooligosaccharide--protein
1194 glycosyltransferase subunit; N-glycan processing- *Fh*-GCNT2=N-acetyllactosaminide beta-
1195 1,6-N-acetylglucosaminyl-transferase, *Fh*-FUT8=alpha-(1,6)-fucosyltransferase,
1196 B4GALT=beta-1,4-galactosyltransferase, B4GALTNT=Beta--n-
1197 acetylgalactosaminyltransferase, EDEM1=ER degradation-enhancing alpha-mannosidase-
1198 like protein, UGGT= UDP-glucose:glycoprotein glucosyltransferase, MAN2B1=alpha-
1199 mannosidase.

1200 **S6. Table. (A) identified miRNAs (B) novel miRNAs (C) differentially expressed**
1201 **miRNAs (D) miRNA regulated Wnt genes**

1202

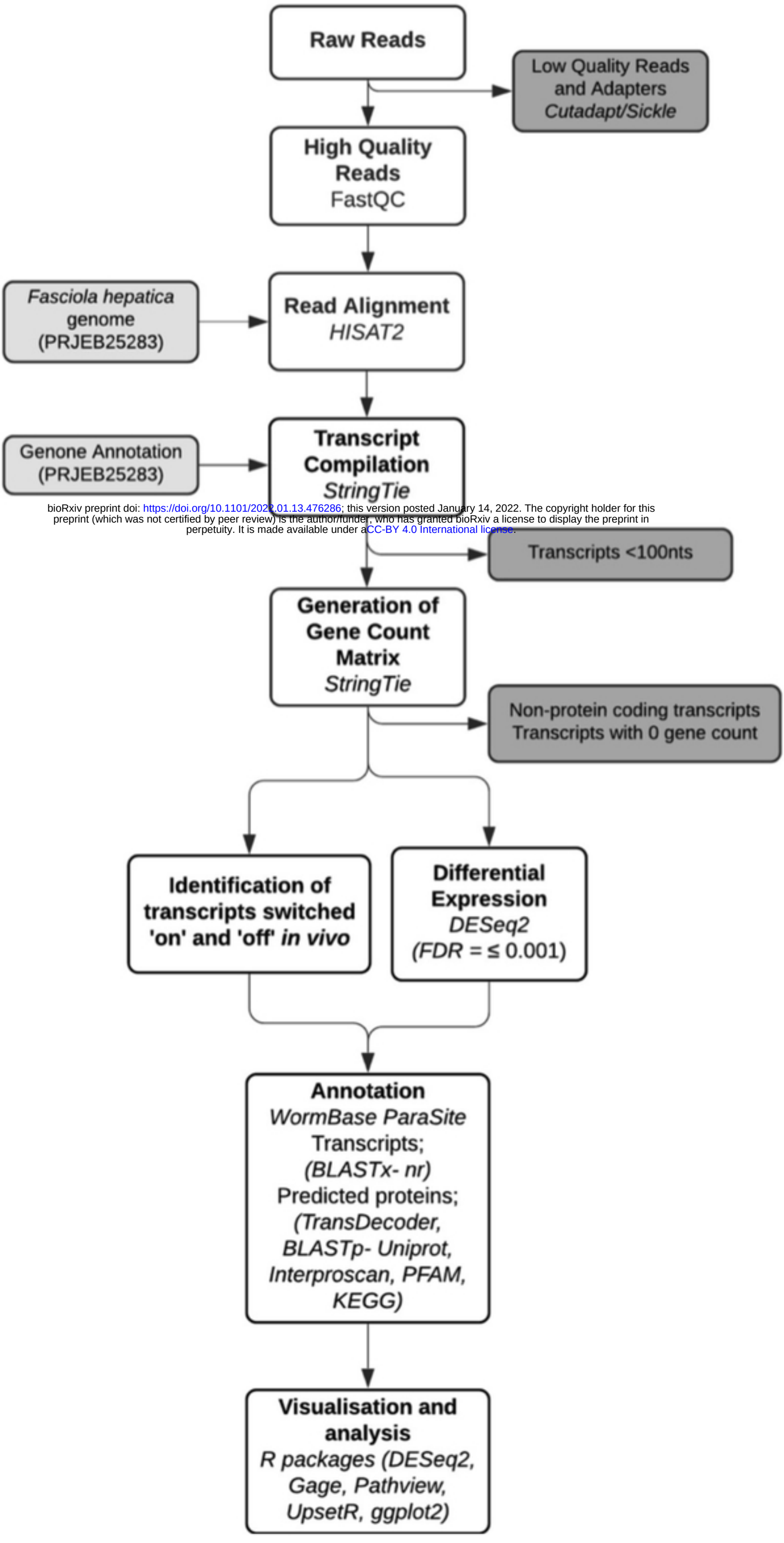

Figure 1

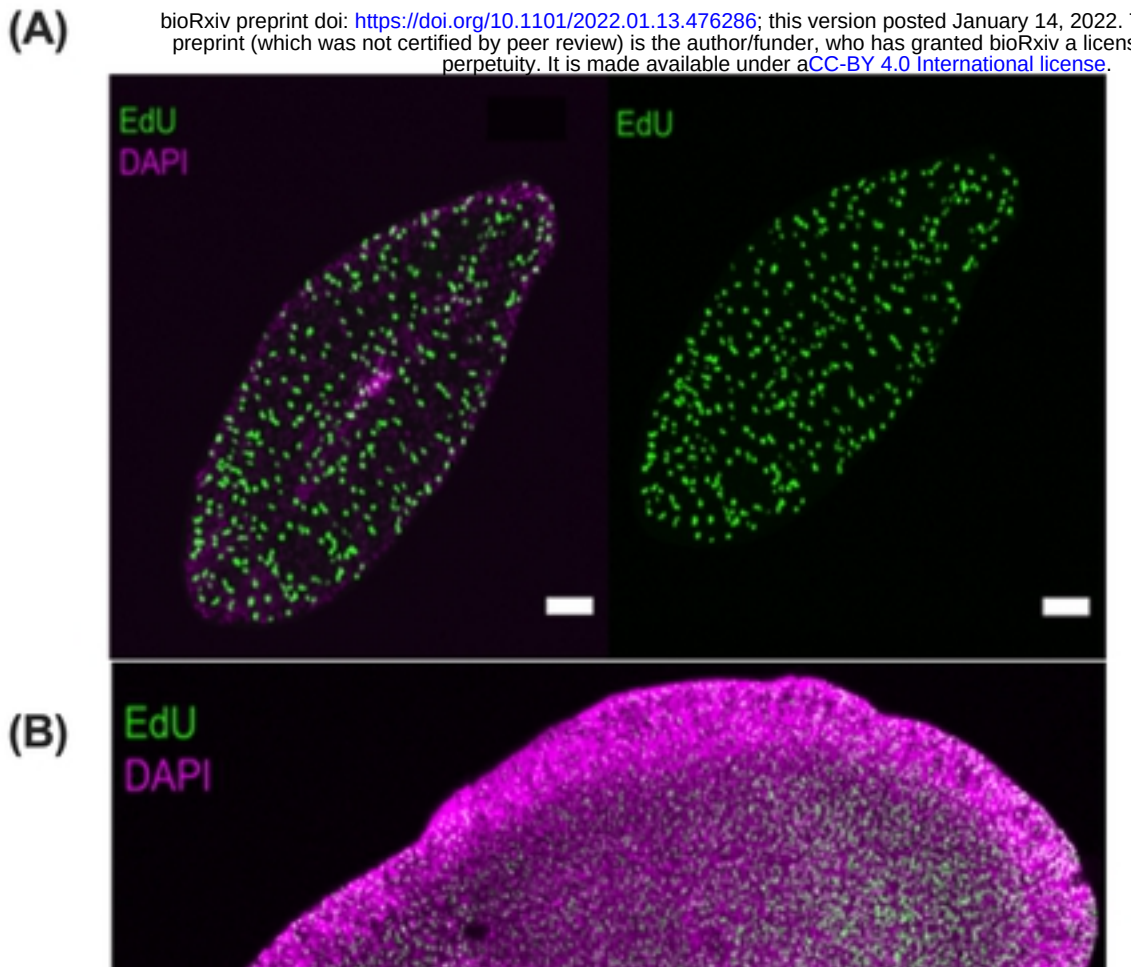

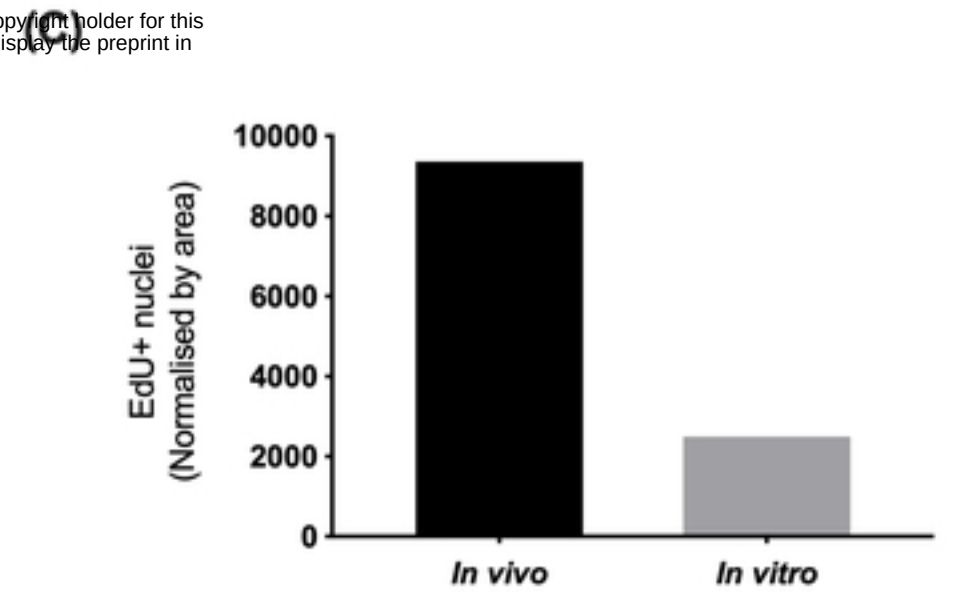

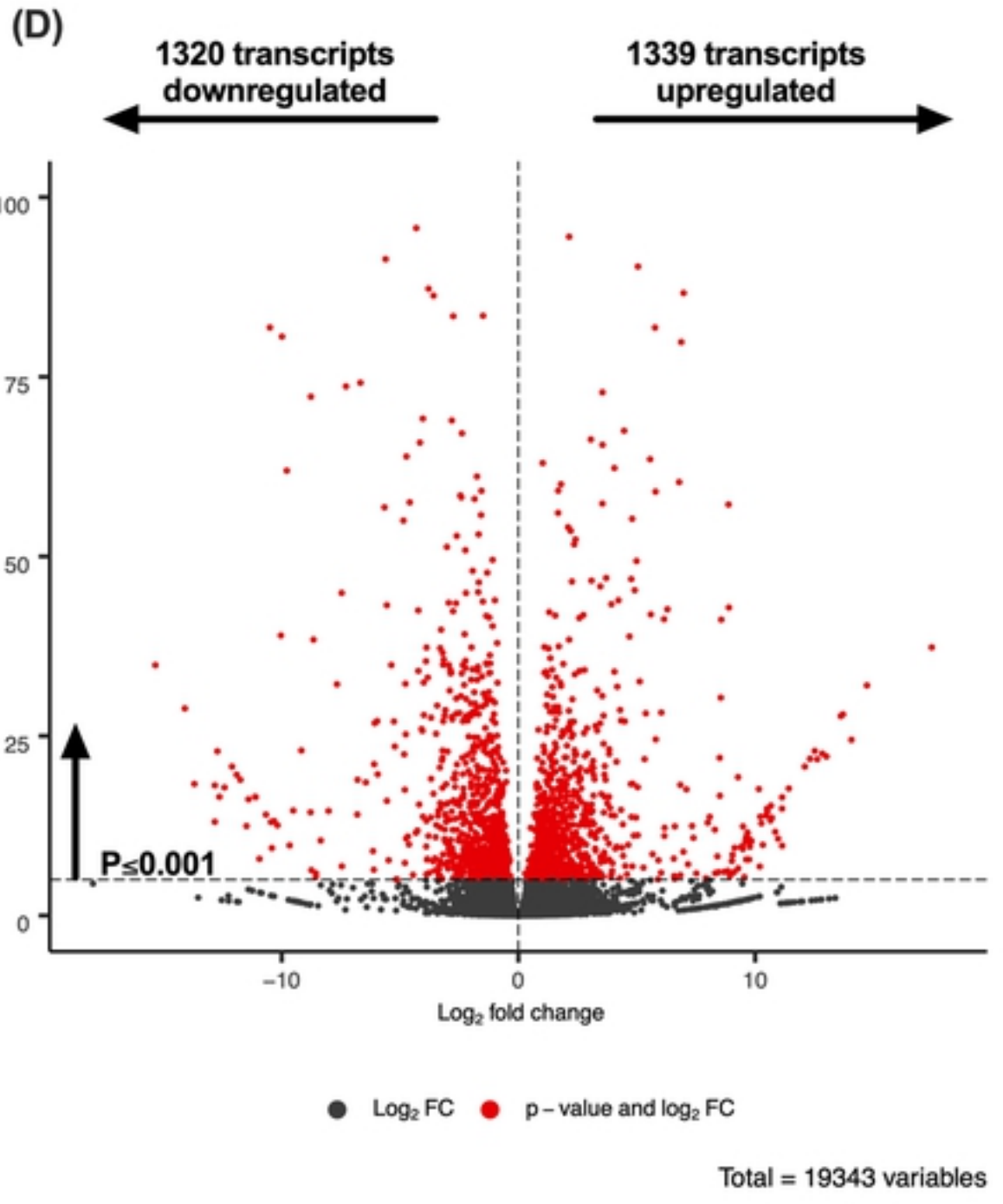

Figure 2

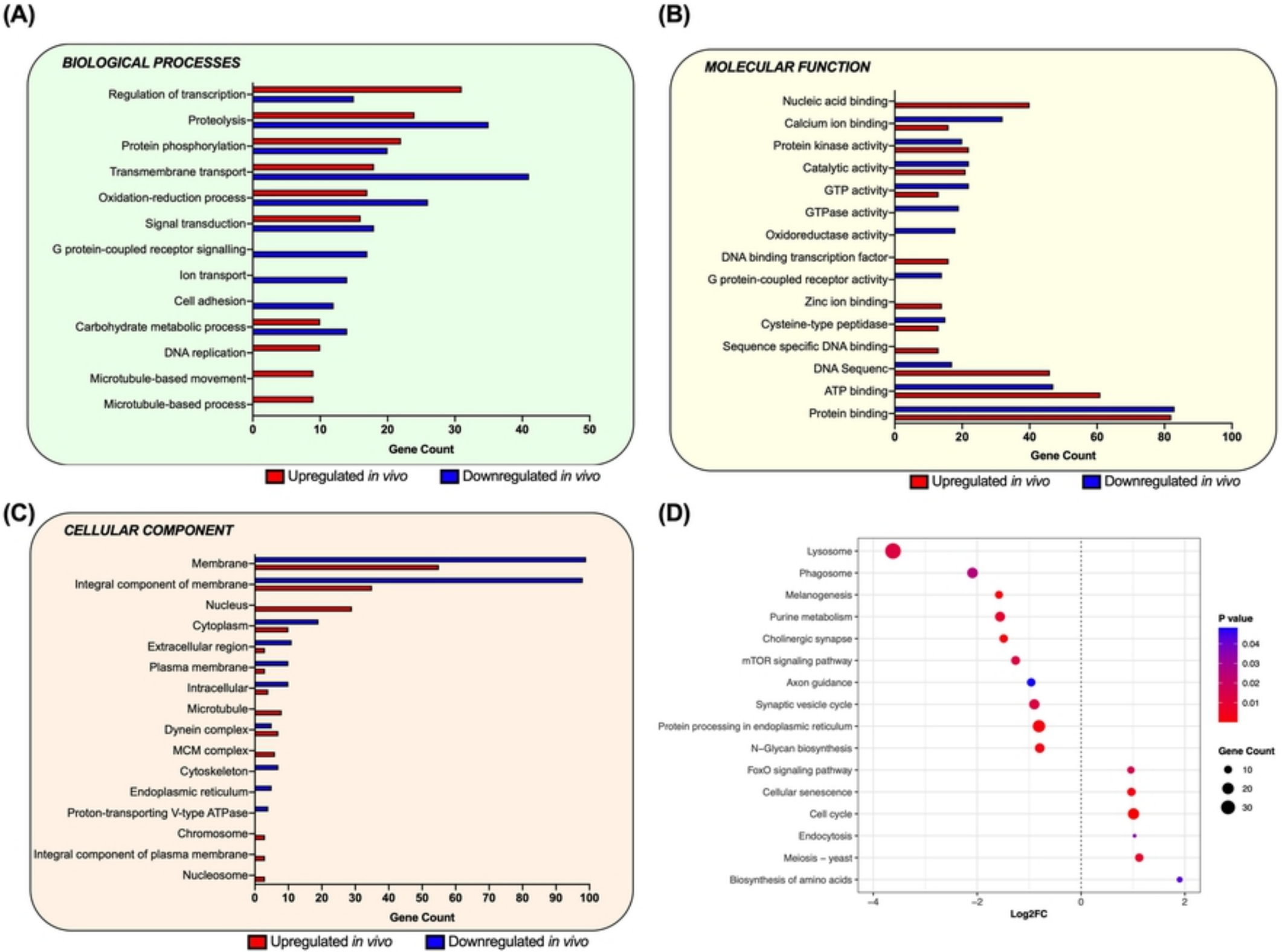
(A)
BIOLOGICAL PROCESSES
Regulation of transcription
Proteolysis
Protein phosphorylation
Transmembrane transport
Oxidation-reduction process
Signal transduction
G protein-coupled receptor signalling
Ion transport
Cell adhesion
Carbohydrate metabolic process
DNA replication
Microtubule-based movement
Microtubule-based process
0 10 20 30 40 50
Gene Count
Upregulated in vivo
Downregulated in vivo
(B)
MOLECULAR FUNCTION
Nucleic acid binding
Calcium ion binding
Protein kinase activity
Catalytic activity
GTP activity
GTPase activity
Oxidoreductase activity
DNA binding transcription factor
G protein-coupled receptor activity
Zinc ion binding
Cysteine-type peptidase
Sequence specific DNA binding
DNA Sequenc
ATP binding
Protein binding
0 20 40 60 80 100
Gene Count
Upregulated in vivo
Downregulated in vivo
(C)
CELLULAR COMPONENT
Membrane
Integral component of membrane
Nucleus
Cytoplasm
Extracellular region
Plasma membrane
Intracellular
Microtubule
Dynein complex
MCM complex
Cytoskeleton
Endoplasmic reticulum
Proton-transporting V-type ATPase
Chromosome
Integral component of plasma membrane
Nucleosome
0 10 20 30 40 50 60 70 80 90 100
Gene Count
Upregulated in vivo
Downregulated in vivo
(D)
Lysosome
Phagosome
Melanogenesis
Purine metabolism
Cholinergic synapse
mTOR signaling pathway
Axon guidance
Synaptic vesicle cycle
Protein processing in endoplasmic reticulum
N−Glycan biosynthesis
FoxO signaling pathway
Cellular senescence
Cell cycle
Endocytosis
Meiosis − yeast
Biosynthesis of amino acids
−4 −2 0 2
Log2FC
P value
0.04
0.03
0.02
0.01
Gene Count
10
20
30

Figure 3

(A)

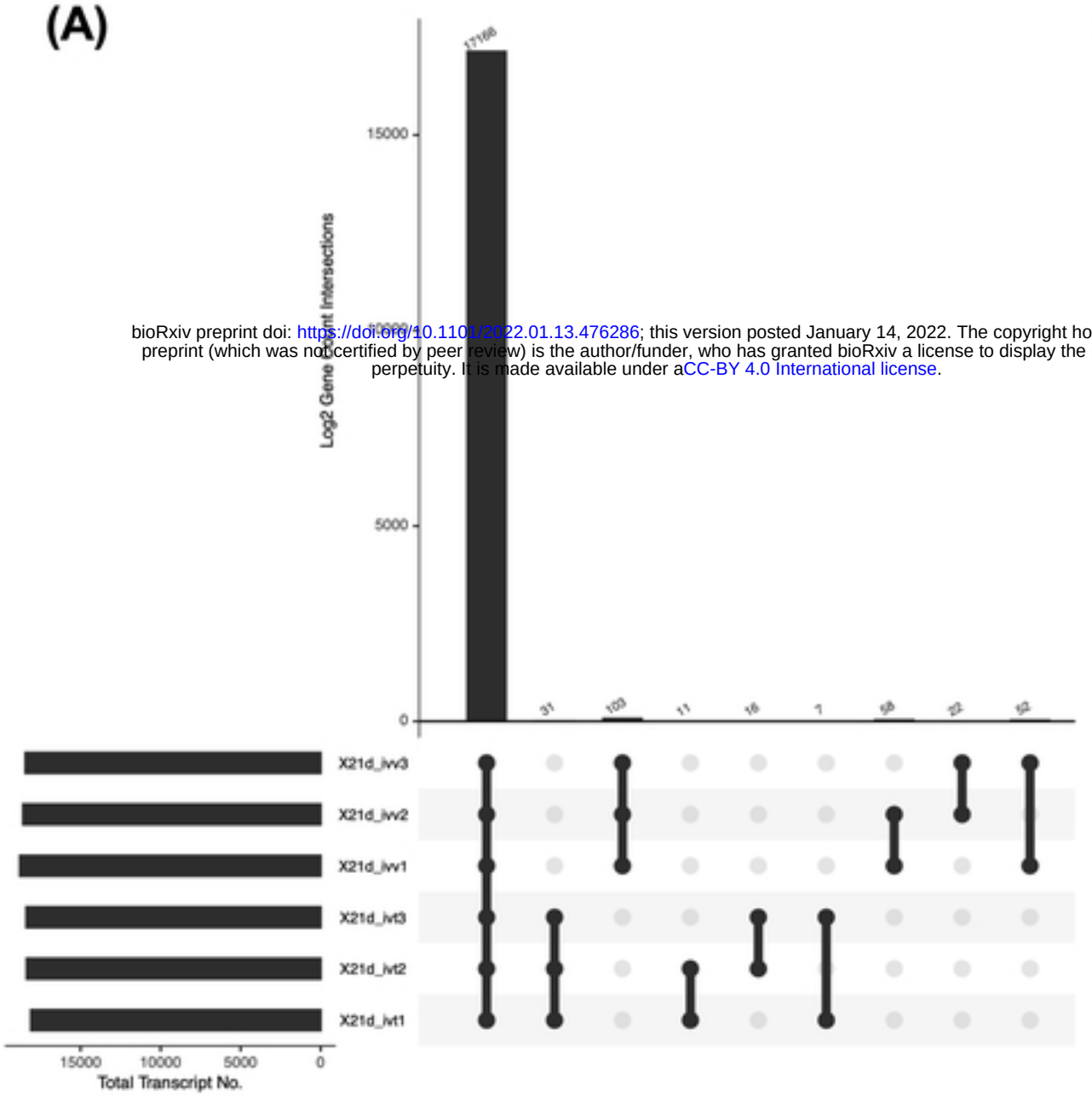

(B)

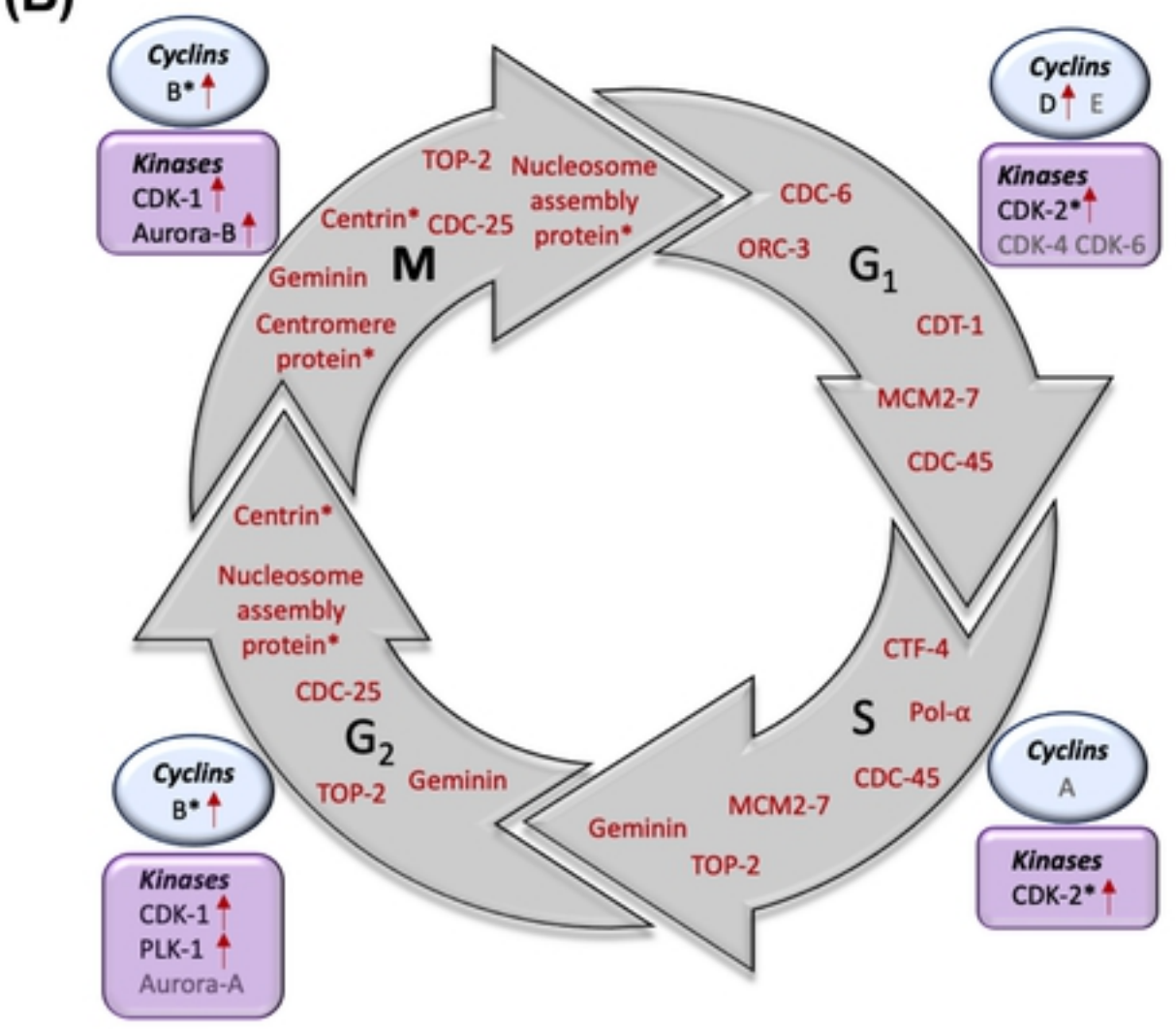

(C)

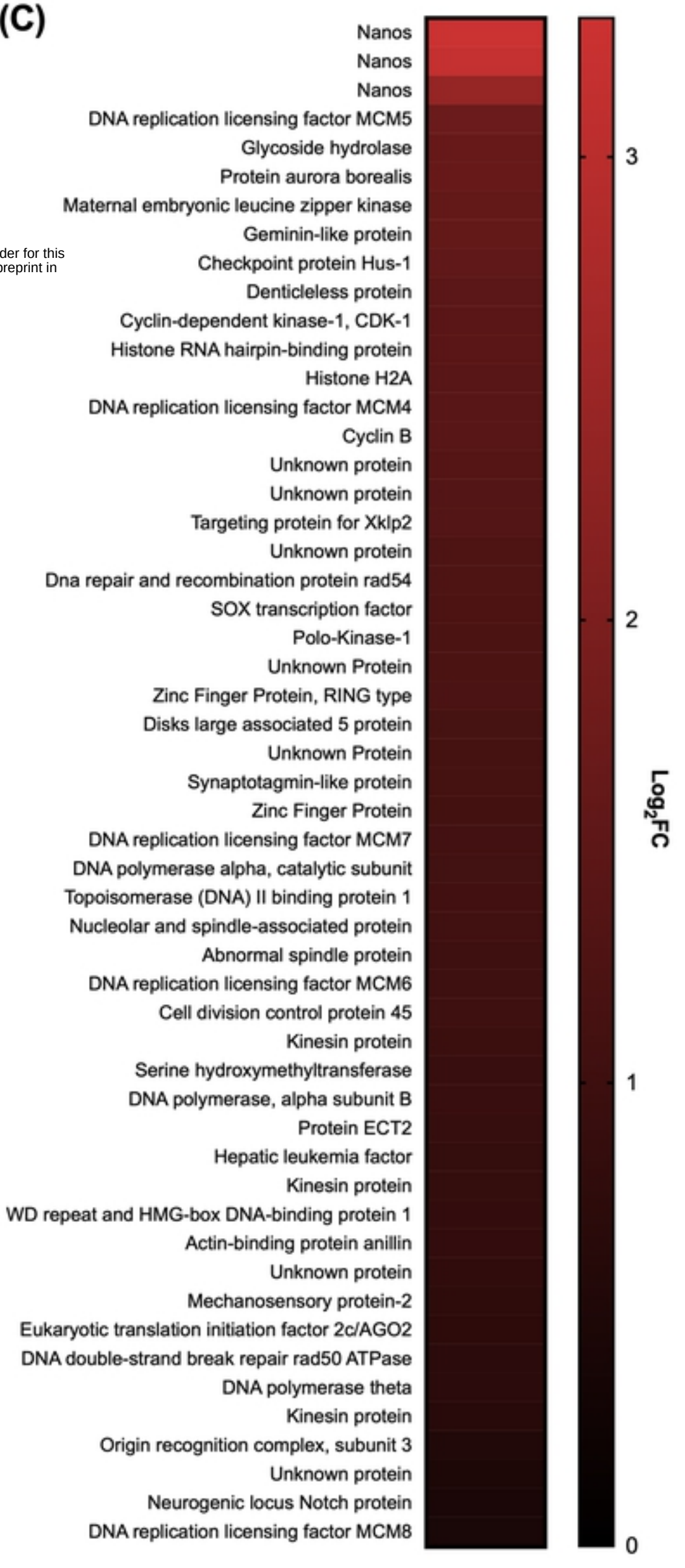

Figure 4

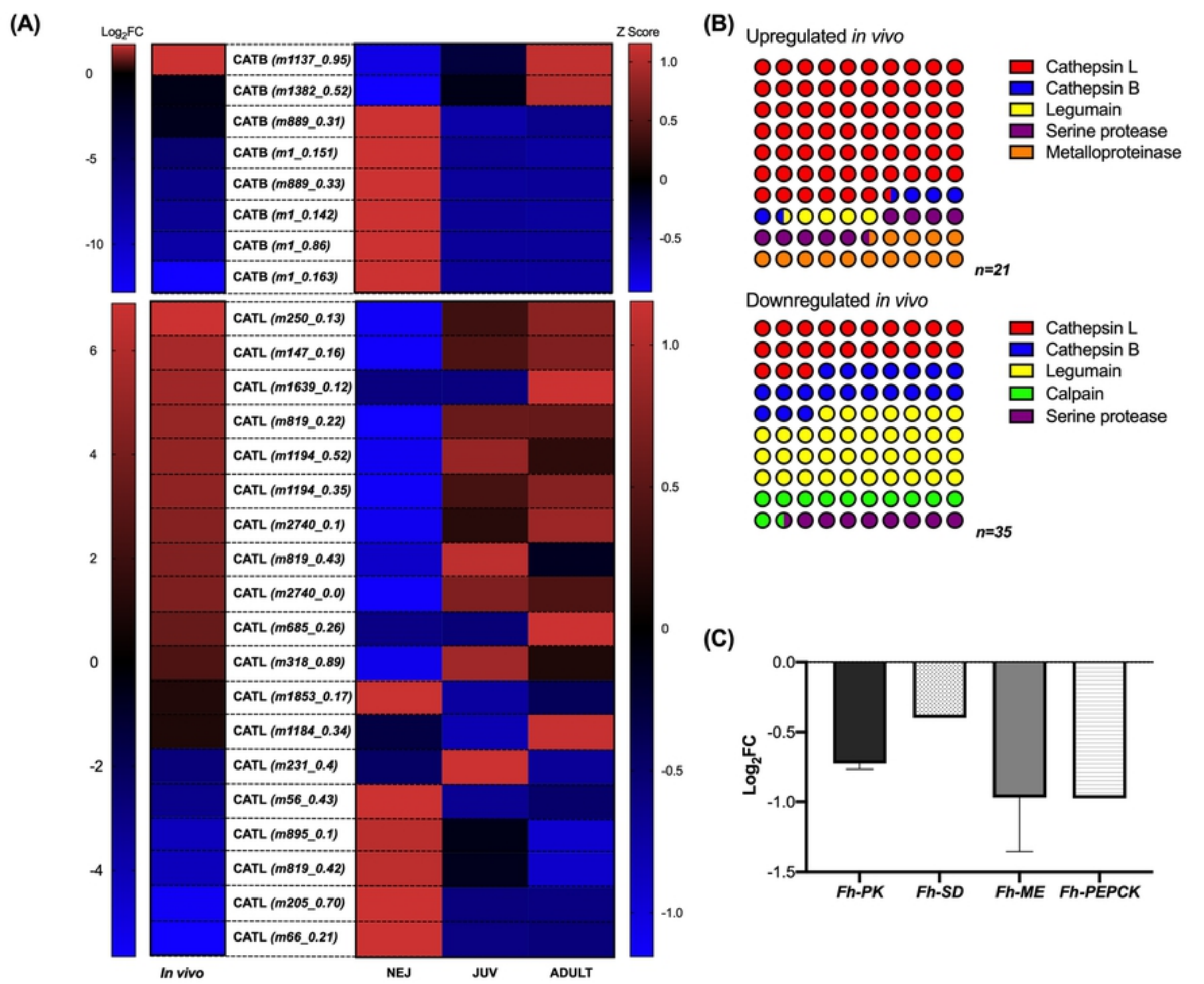
(A)
Log2FC
Z Score
CATB (m1137_0.95)
CATB (m1382_0.52)
CATB (m889_0.31)
CATB (m1_0.151)
CATB (m889_0.33)
CATB (m1_0.142)
CATB (m1_0.86)
CATB (m1_0.163)
CATL (m250_0.13)
CATL (m147_0.16)
CATL (m1639_0.12)
CATL (m819_0.22)
CATL (m1194_0.52)
CATL (m1194_0.35)
CATL (m2740_0.1)
CATL (m819_0.43)
CATL (m2740_0.0)
CATL (m685_0.26)
CATL (m318_0.89)
CATL (m1853_0.17)
CATL (m1184_0.34)
CATL (m231_0.4)
CATL (m56_0.43)
CATL (m895_0.1)
CATL (m819_0.42)
CATL (m205_0.70)
CATL (m66_0.21)
In vivo
NEJ
JUV
ADULT
(B)
Upregulated in vivo
Cathepsin L
Cathepsin B
Legumain
Serine protease
Metalloproteinase
n=21
Downregulated in vivo
Cathepsin L
Cathepsin B
Legumain
Calpain
Serine protease
n=35
(C)
Log2FC
Fh-PK
Fh-SD
Fh-ME
Fh-PEPCK

Figure 5

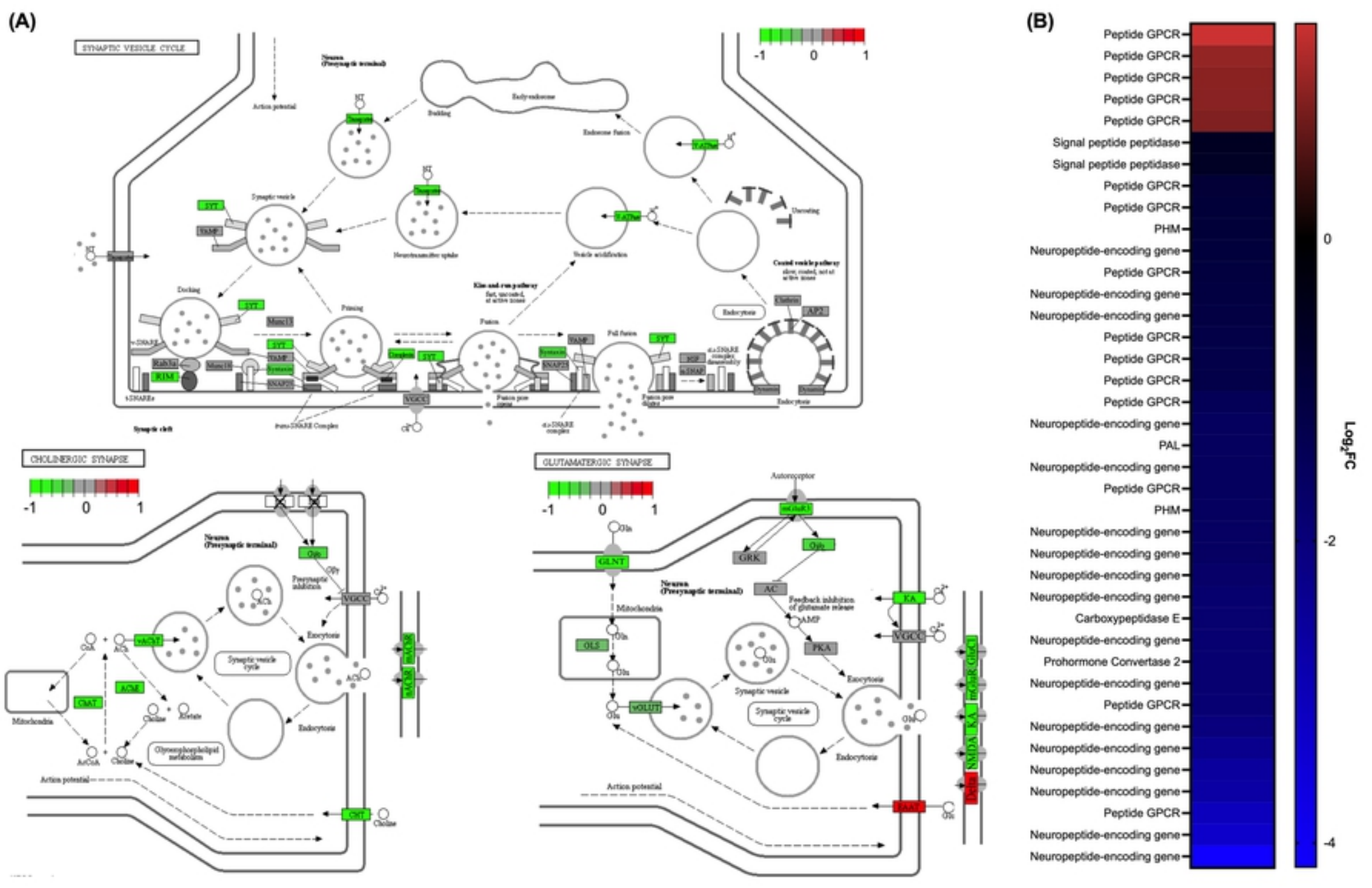
(A)
SYNAPTIC VESICLE CYCLE
CHOLINERGIC SYNAPSE
GLUTAMATERGIC SYNAPSE
(B)
Peptide GPCR
Peptide GPCR
Peptide GPCR
Peptide GPCR
Peptide GPCR
Signal peptide peptidase
Signal peptide peptidase
Peptide GPCR
Peptide GPCR
PHM
Neuropeptide-encoding gene
Peptide GPCR
Neuropeptide-encoding gene
Neuropeptide-encoding gene
Peptide GPCR
Peptide GPCR
Peptide GPCR
Peptide GPCR
Peptide GPCR
Neuropeptide-encoding gene
PAL
Neuropeptide-encoding gene
Peptide GPCR
PHM
Neuropeptide-encoding gene
Neuropeptide-encoding gene
Neuropeptide-encoding gene
Neuropeptide-encoding gene
Neuropeptide-encoding gene
Carboxypeptidase E
Neuropeptide-encoding gene
Prohormone Convertase 2
Neuropeptide-encoding gene
Peptide GPCR
Neuropeptide-encoding gene
Neuropeptide-encoding gene
Neuropeptide-encoding gene
Neuropeptide-encoding gene
Peptide GPCR
Neuropeptide-encoding gene
Neuropeptide-encoding gene
0
-2
-4
Log2FC

Figure 6

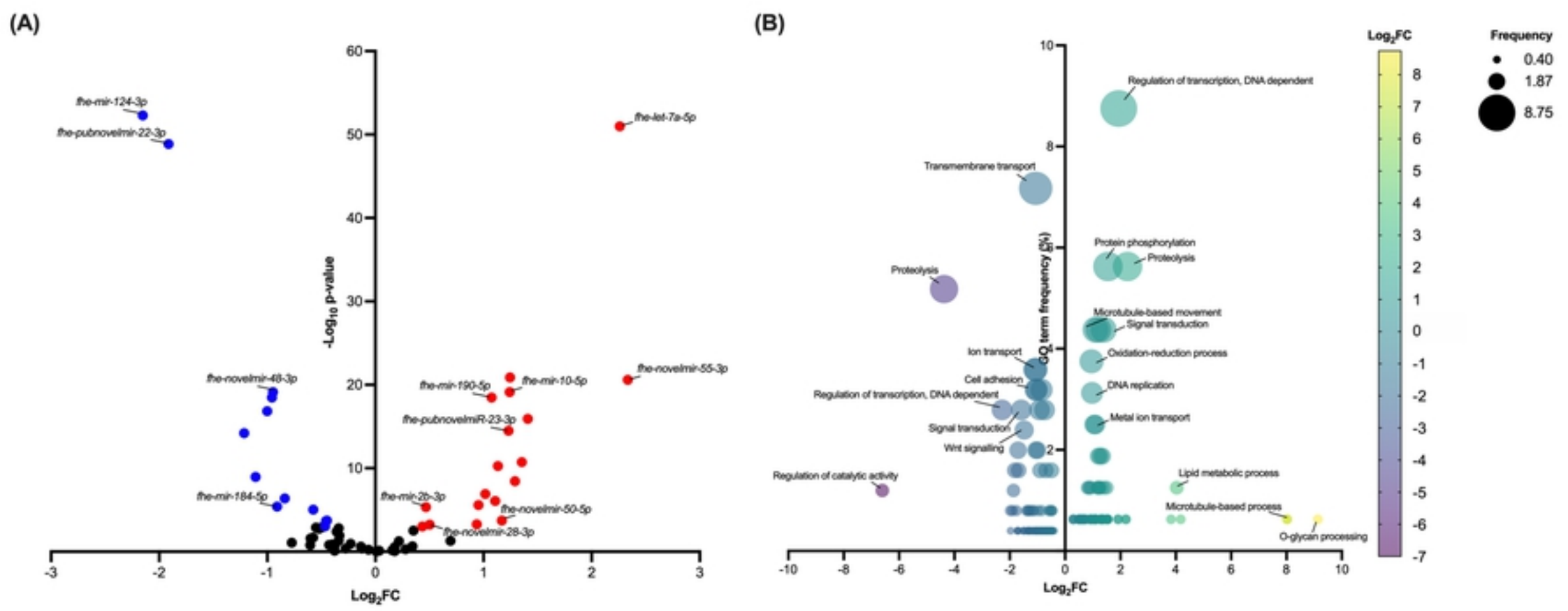
(A)
fhe-mir-124-3p
fhe-pubnovelmir-22-3p
fhe-let-7a-5p
fhe-novelmir-55-3p
fhe-novelmir-48-3p
fhe-mir-190-5p
fhe-mir-10-5p
fhe-pubnovelmiR-23-3p
fhe-mir-184-5p
fhe-mir-2b-3p
fhe-novelmir-50-5p
fhe-novelmir-28-3p
-Log10 p-value
Log2FC
(B)
Log2FC
Frequency
0.40
1.87
8.75
Regulation of transcription, DNA dependent
Transmembrane transport
Protein phosphorylation
Proteolysis
Microtubule-based movement
Signal transduction
Oxidation-reduction process
Ion transport
Cell adhesion
DNA replication
Regulation of transcription, DNA dependent
Metal ion transport
Signal transduction
Wnt signalling
Regulation of catalytic activity
Lipid metabolic process
Microtubule-based process
O-glycan processing
GO term frequency (%)
Log2FC

Figure 7